Laser-Plasma Physics Probed by Protons

Andrea Macchi

CNR/INFM/polyLAB, Pisa
Dipartimento di Fisica "Enrico Fermi", Università di Pisa

www.df.unipi.it/~macchi/

CLPU, Universidad de Salamanca, January 13, 2010

Main contributors

Francesco Ceccherini, Fulvio Cornolti,
Francesco Pegoraro
Dipartimento di Fisica "Enrico Fermi",
Università di Pisa and CNISM, Pisa

Tatiana V. Liseykina
Institute of Computer Technologies,
SD-RAS, Novosibirsk, Russia and
MPI-K, Heidelberg, Germany

Alessandra Bigongiari*, Carlo Alberto Cecchetti,
Satyabrata Kar, Kevin E. Quinn, Lorenzo Romagnani,
Marco Borghesi
School of Mathematics and Physics,
Queen's University, Belfast, UK

**presently at Ecole Polytechnique, France*

Outline

- Laser-Accelerated Protons as a probe of Laser-Plasma interactions
- Proton probing-based investigations
  - ➔ Plasma expansion and sheath acceleration
  - ➔ Pulse self-channeling in the charge-displacement regime
  - ➔ Ultrafast charging dynamics

The discovery of MeV proton emission in superintense interaction with *metallic* targets

Reported in 2000
by three experimental groups

[Clark et al, PRL **84** (2000) 670;
Maksimchuk et al, *ibid.*, 4108;
Snavely et al, PRL 85 (2000) 2945*

*** - 2 X 10^{13} protons with energy > 10 MeV,**
58 MeV cut-off,
good collimation (20°)
conversion efficiency
12% of laser energy
@ I=3 x 10^{20} W/cm^2

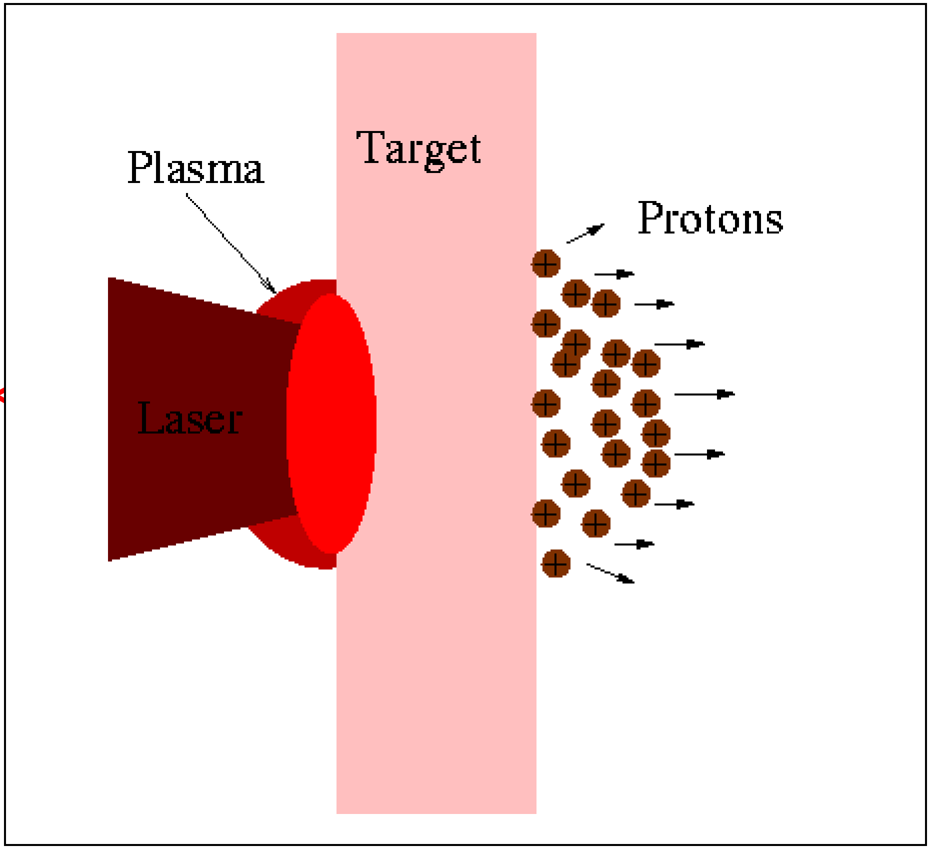

The discovery of MeV proton emission in superintense interaction with *metallic* targets

Reported in 2000
by three experimental groups

[Clark et al, PRL **84** (2000) 670;
Maksimchuk et al, *ibid.*, 4108;
Snavely et al, PRL 85 (2000) 2945*

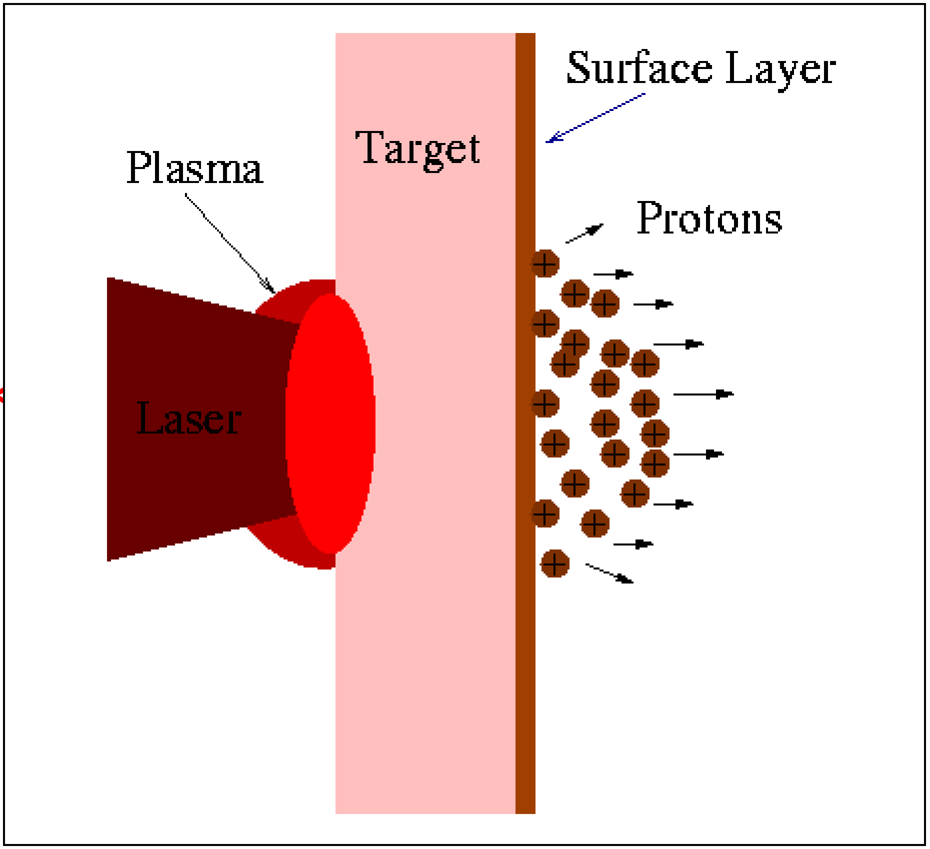

*** - 2 X 10^{13} protons with energy > 10 MeV,**
58 MeV cut-off,
good collimation (20°)
conversion efficiency
12% of laser energy
@ I=3 x 10^{20} W/cm^2

Question: origin of protons from metal?

Answer: hydrocarbon or water impurities
on the target surface
(e.g. from vacuum pump ...)

The discovery of MeV proton emission in superintense interaction with *metallic* targets

Reported in 2000
by three experimental groups

[Clark et al, PRL **84** (2000) 670;
Maksimchuk et al, *ibid.*, 4108;
<u>Snavely et al, PRL 85 (2000) 2945</u>*

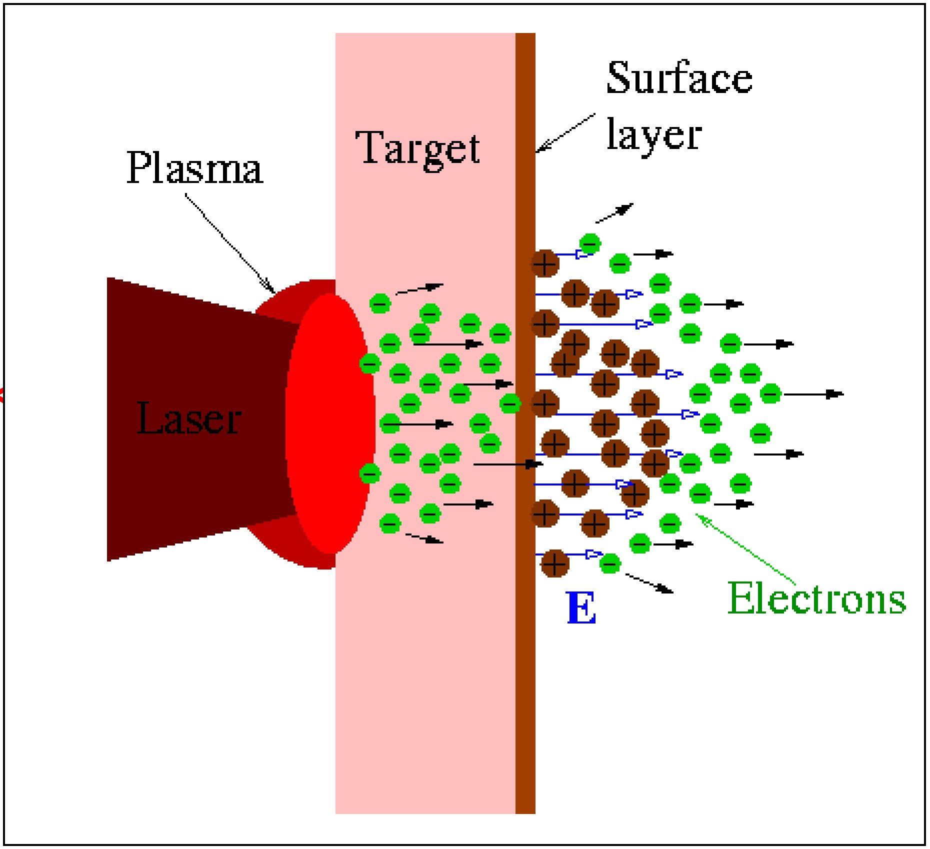

*** - 2 X 10^{13} protons with energy > 10 MeV,
58 MeV cut-off,
good collimation (20°)
conversion efficiency
12% of laser energy
@ I=3 x 10^{20} W/cm^2**

Physical mechanism:
acceleration in the space-charge electric field generated by "fast" electrons escaping from the target
(TNSA, Target Normal Sheath Acceleration)

TNSA (Target Normal Sheath Acceleration) model

After an intense debate on the Origin of Protons
(*more in the following*...)
TNSA has been accepted as the basic
mechanism leading to proton acceleration in most of the reported experiments and provided a framework for source development and optimization

Schwoerer et al, Nature **439** (2006) 445
Hegelich et al, Nature **439** (2006) 441
Toncian et al, Science **312** (2006) 410
Fuchs et al, Nature Physics **2** (2005) 48
Robson et al, Nature Physics **3** (2007) 58
Kar et al, PRL **100** (2008) 105004

The TNSA picture accounts for the observed properties of the proton source

[picture from S. Wilks et al,
Phys. Plasmas **8** (2001) 542]

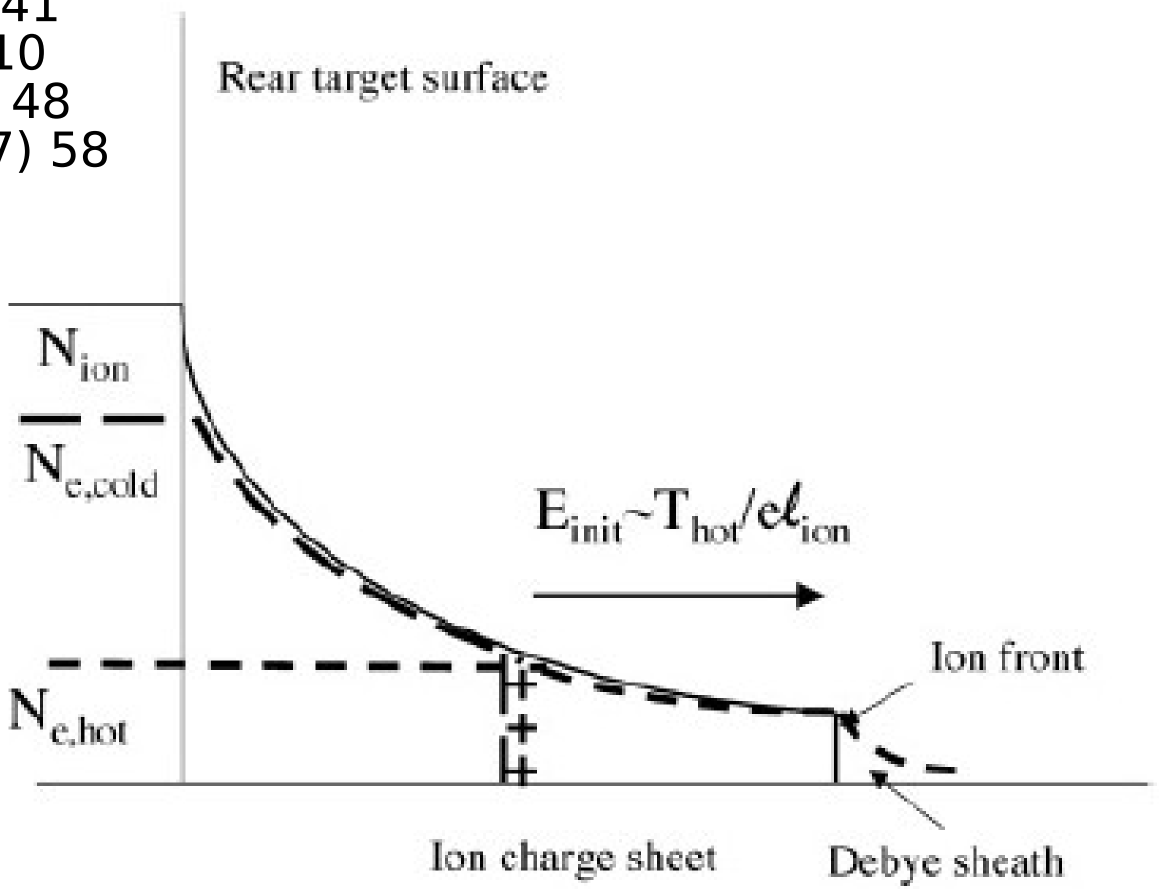

Use of laser-accelerated protons as a probe of EM fields in laser-plasma interactions

Due to high laminarity the proton beam has **imaging properties**

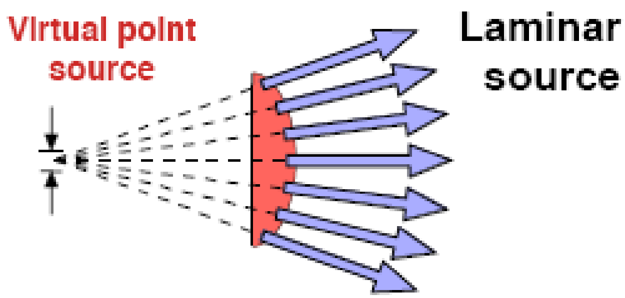

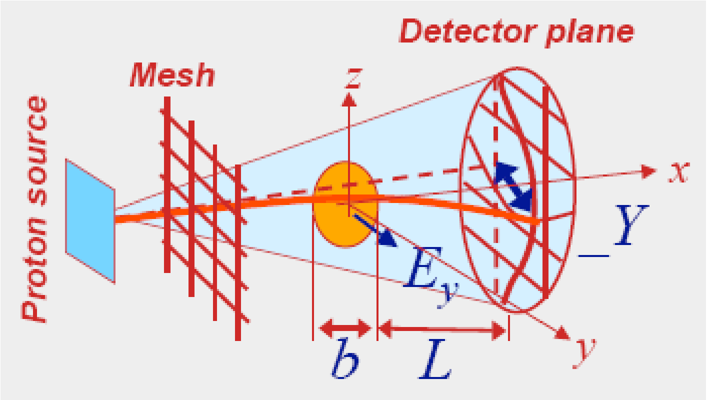

The short duration of the proton burst allows **picosecond temporal resolution**

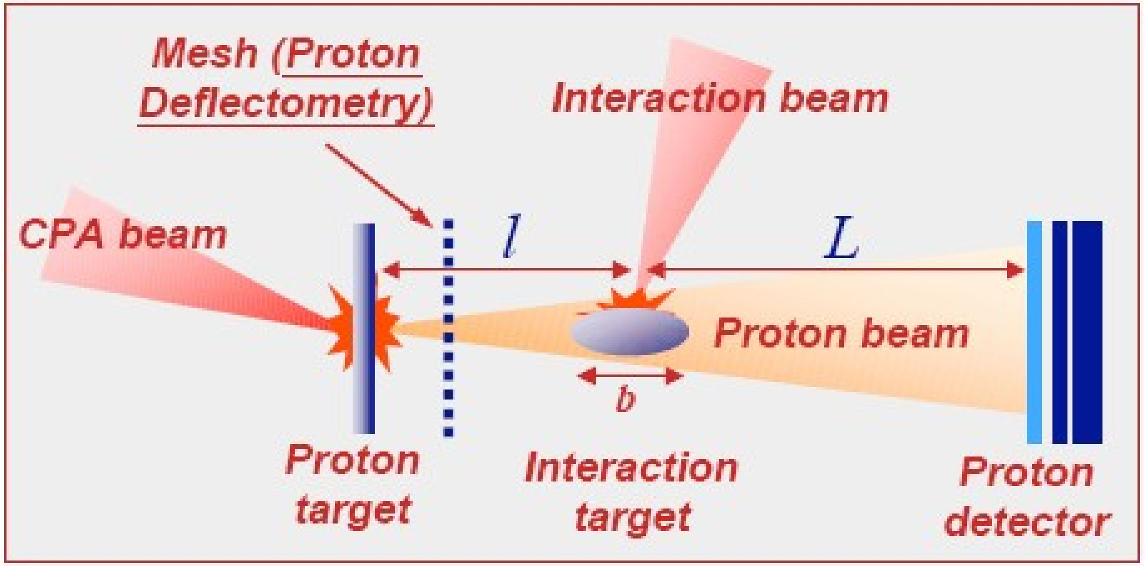

Protons of a given energy will cross the probed object at a particular time.
An energy-resolving detector (e.g. Radiochromic Film) thus provides **multiframe capability**

Borghesi et al, Phys.Plasmas **9** (2002) 2214
Borghesi et al, Phys.Rev.Lett. **92** (2004) 055003
Cowan et al, Phys.Rev.Lett. **92** (2004) 204851

In a laser-plasma experiment the proton probe is easily **synchronized with the interaction**

Properties of the proton source

Imaging properties of the emitted protons are those of a **point-like virtual source**

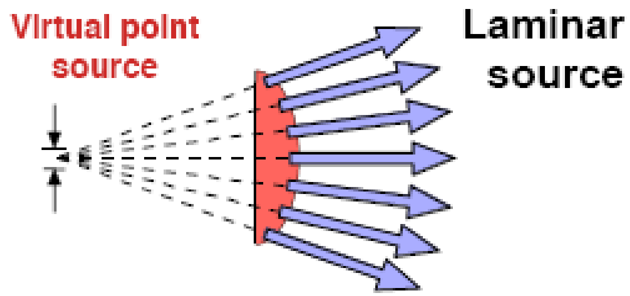

Proton beam is **quasi-laminar** (**ultra-low emittance**)

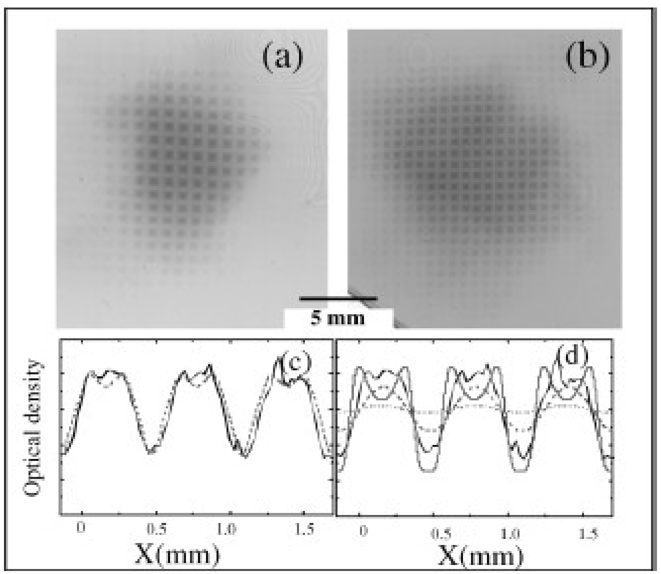

μ m grid mesh image

Shadow of micrometric grid mesh with 15 MeV protons provides magnification test and estimate of source dimensions $a < 10\ \mu m$
[Borghesi et al, PRL **92** (2004) 055003]

$a = 1.4\ \mu m$ reported at lower energy
[Cobble et al, J.Appl.Phys. **92** (2002) 1775]

Imaging of thin objects possible due to multiple small-angle scattering of protons
[West & Sherwood, Nature **239** (1972) 157]

Transverse emittance measurement for >10 MeV protons
[Cowan et al, PRL **92** (2004) 204801]

$\epsilon < 4 \times 10^{-3}$ mm mrad

Energy resolving allows temporal resolution

Use of RadioChromic Film (RCF) stack as a detector allows single-shot, spatial and **energy** resolution of the proton beam

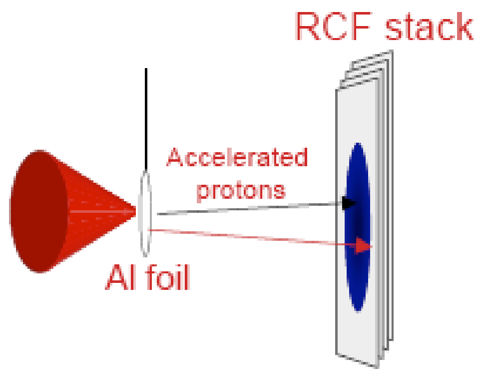

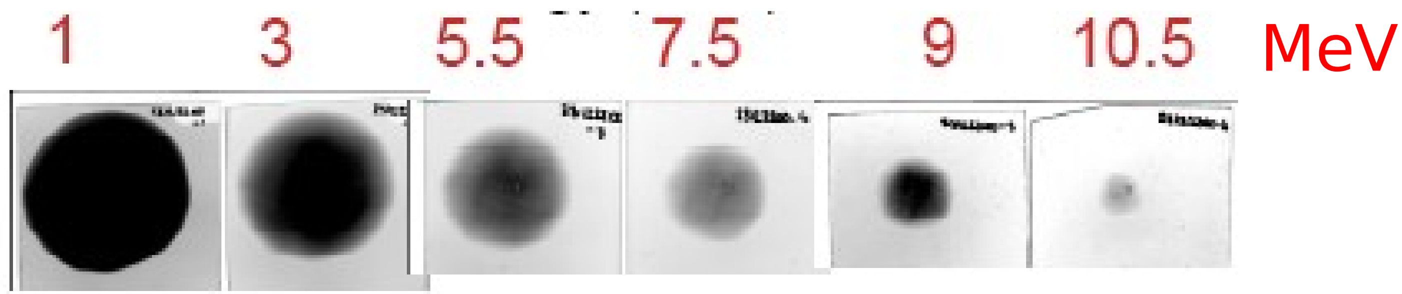

Typical data example

(taken at the LULI 100 TW facility, École Polytechnique, Palaiseau, France)

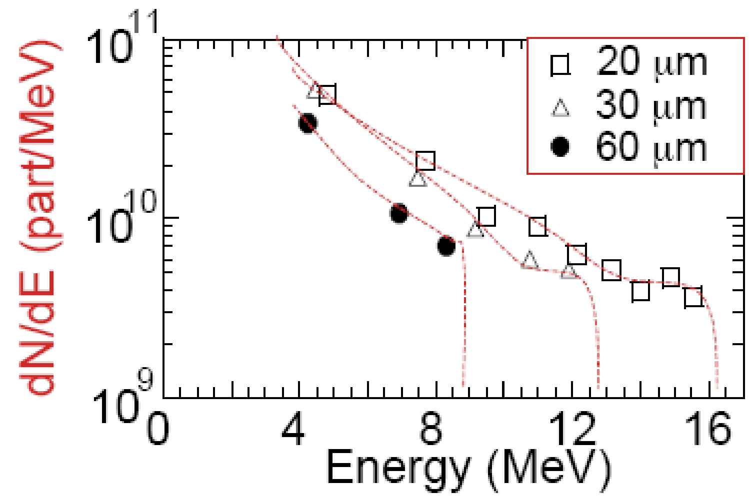

RCF energy selection capability is a consequence of Bragg peak deposition

Energy resolving allows temporal resolution

Use of RadioChromic Film (RCF) stack as a detector allows single-shot, spatial and **energy** resolution of the proton beam

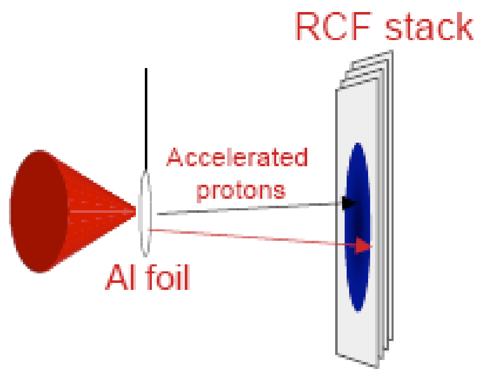

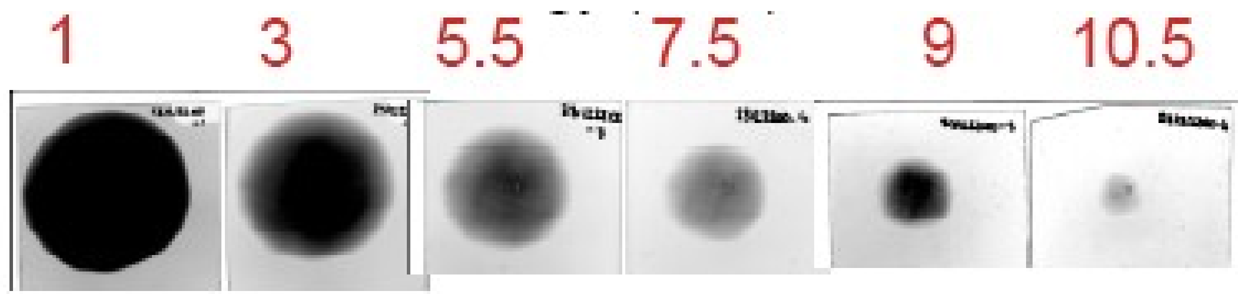

MeV

72 42 31 26 24 22 ps

In a time-of-flight arrangement protons of different energies cross the object at different times: imaging of transient objects possible

RCF energy bandwidth allows picosecond resolution

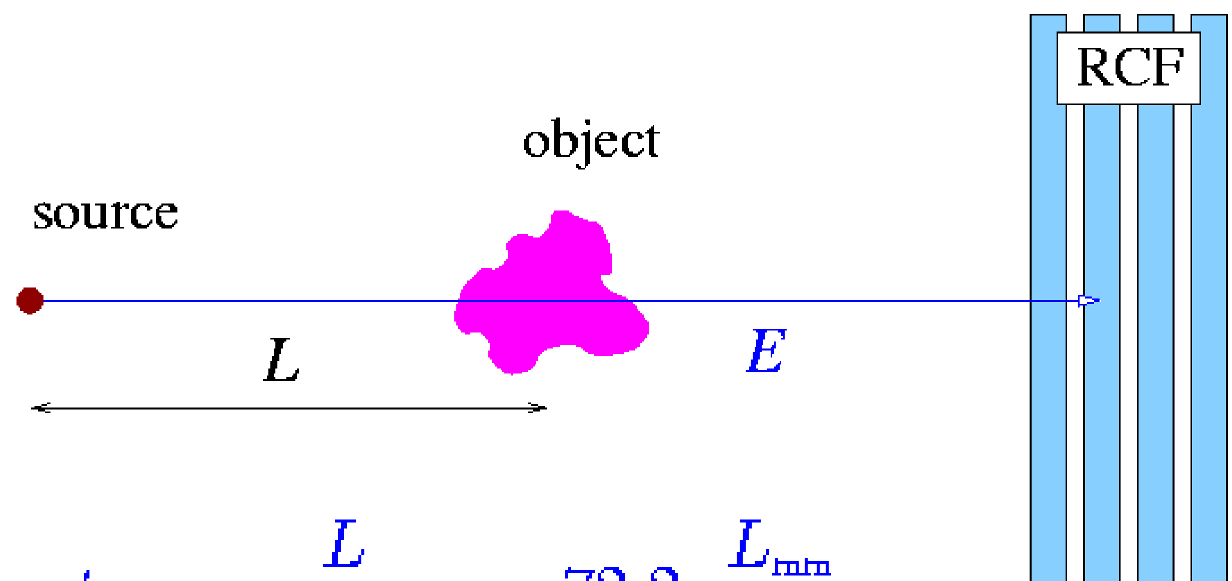

$$t_p = \frac{L}{\sqrt{2E/m_p}} = 72.2 \frac{L_{\mathrm{mm}}}{\sqrt{E_{\mathrm{MeV}}}} \mathrm{ps}$$

Using protons to detect EM fields

A proton crossing an EM field distribution acquires a transverse velocity $\delta\ \mathbf{v}$

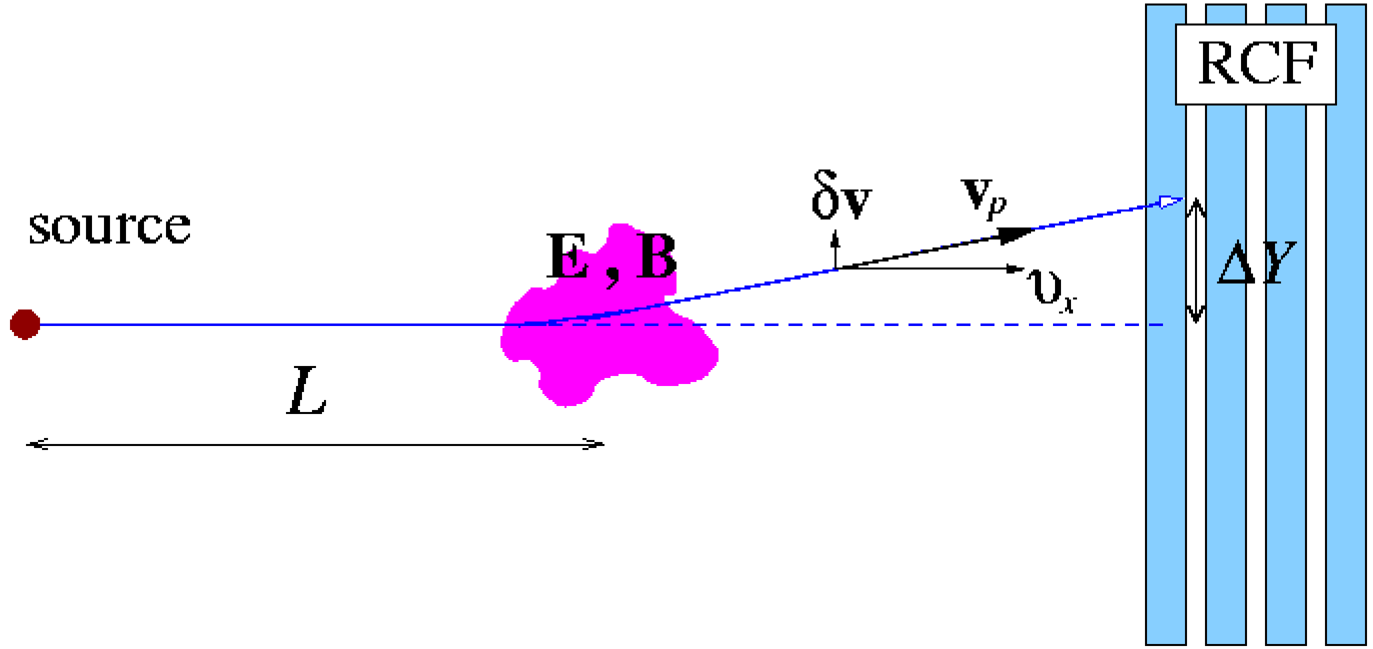

$$\delta\mathbf{v} = \frac{e}{m_p}\int (\mathbf{E} + \mathbf{v}_p \times \mathbf{B})\, dt$$

For *weak* deflections (1st order Born approximation)

$$v_x = \frac{dx}{dt} \simeq v_p \quad \rightarrow \quad \delta Y = |\delta\mathbf{v}_\perp|\Delta t \simeq \frac{eL}{2\mathcal{E}_p}\int (\mathbf{E} + \mathbf{v}_p \times \mathbf{B})_\perp\, dx$$

Concept: estimate $\mathbf{E}$ (and/or $\mathbf{B}$) from the measurement of $\Delta\ Y$

Proton “Deflectometry”

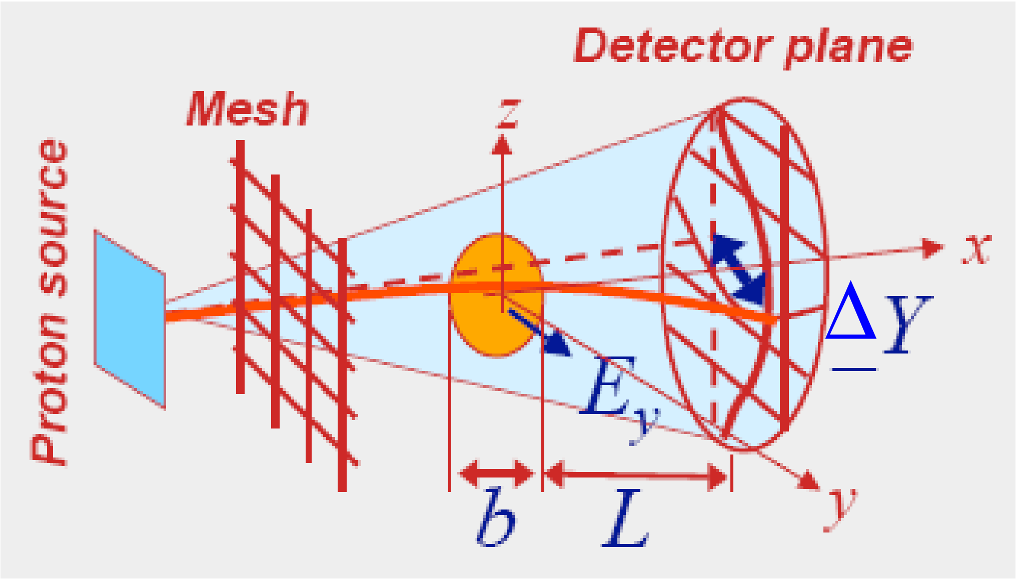

The proton deflection $\Delta\ Y$ can be measured directly by the deformation of the imprint of a stopping mesh

Assuming that only E contributes we estimate the average field as

$$\langle \mathbf{E} \rangle \simeq \frac{1}{b} \int_{-b/2}^{+b/2} \mathbf{E}_\perp dx \simeq \frac{2\mathcal{E}_p}{eLb} \Delta Y$$

Proton "Imaging"

When fields gradients are present deflections produce a modulation δn in the proton density n_p on the detector plane:

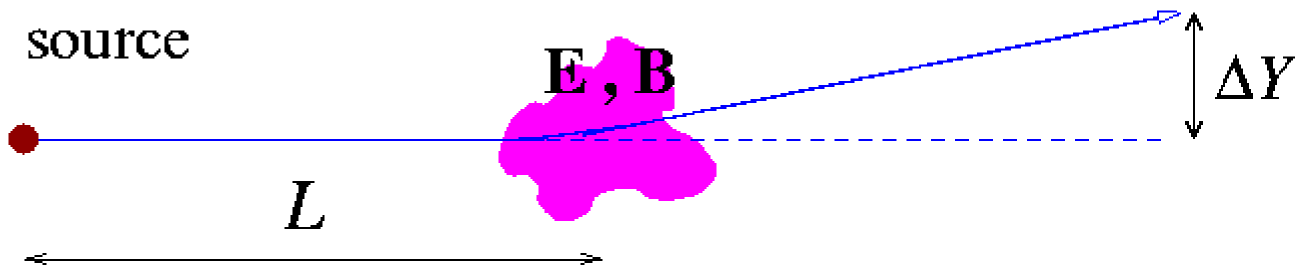

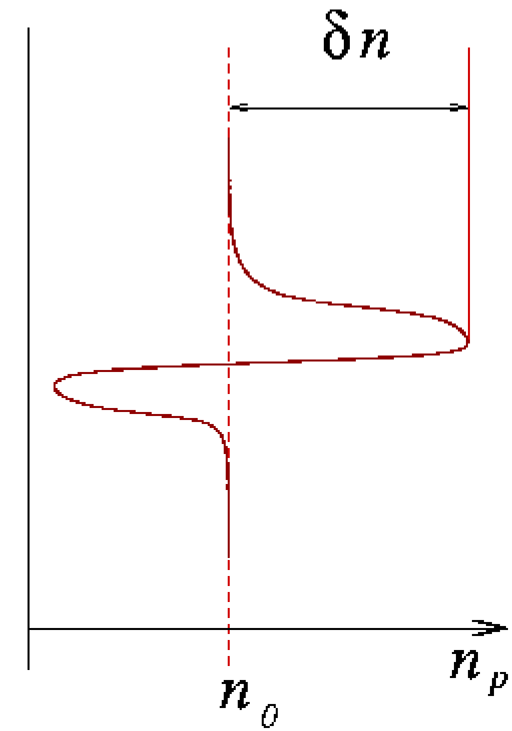

The observed modulation δn is proportional to the line integral of "source" terms

(M : geometrical magnification)

$$\frac{\delta n}{n_0} \simeq -\frac{1}{M}\nabla_{\perp}\cdot\Delta\mathbf{Y} \simeq -\frac{2\pi e L b}{\mathcal{E}_p M}\int_{-b/2}^{+b/2}\left(\rho - \frac{1}{c^2}\mathbf{v}_p\cdot\mathbf{J}\right)dx$$

If electric fields are dominant δn is proportional to the line integral of the charge density ρ along the proton path.

Breaktroughs and limitations (experimental)

Proton Probing gives an unprecedented possibility to detect electric and magnetic fields with high spatial and temporal resolution in low- and high-density plasmas

However...

- an accurate “tomographic” 3D reconstruction of field patterns is not possible (at least with a single proton beam)

-using a single beam the observed effects cannot be attributed with absolute unambiguity to electric or to magnetic fields alone

- evaluating the spatial and temporal resolution of the technique is not straightforward; several effects need to be considered

-> The experimental data must be interpreted
1) within a theoretical framework (starting assumptions)
2) with the help of numerical modeling of proton probing:
particle tracing simulations with $\mathbf{E}(x,t)$ and/or $\mathbf{B}(x,t)$ as input

Breaktroughs and limitations (theoretical)

Proton Probing allows to observe “plasma physics in action” via self-generated electric and magnetic fields, allowing for the first time to observe a large set of phenomena and validate related theories

However...

- the temporal scale accessible to proton probing (ps) is often much larger than the “fast” scale of the investigated phenomena, whose observation is thus based on “remnants” of the fields

- fully self-consistent “ab initio” simulations (e.g. with PIC codes) in 3D and for spatial and temporal scales corresponding to the experiment are often beyond available (super)computing power

-> Models are needed to bridge the gap within “feasible” (e.g. short-scale, 2D, symmetry assumptions ...) simulations and the experimentally relevant regimes

Working on “proton probing experiments”

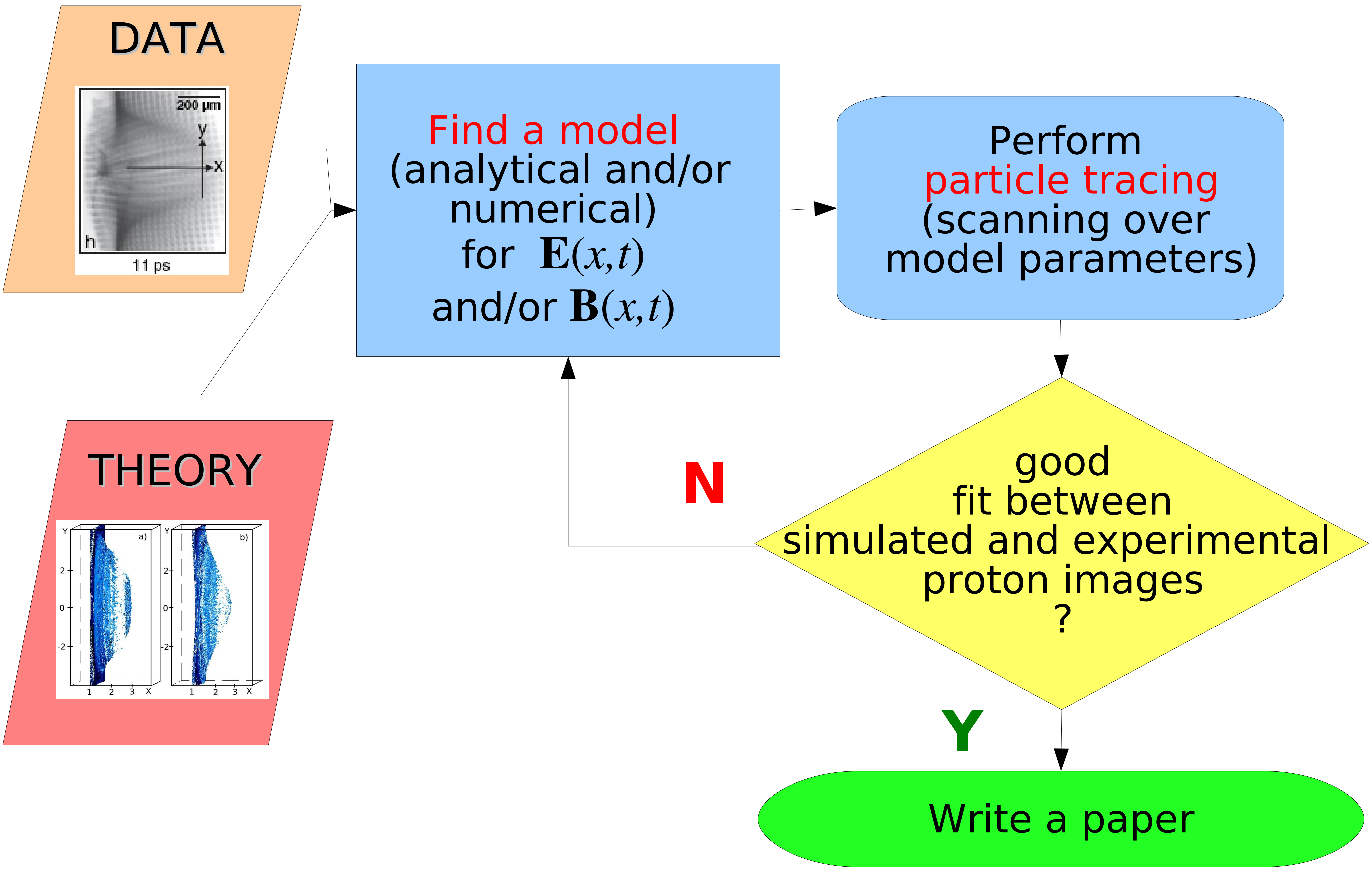

Several basic phenomena observed by proton probing

Bubble-like structures interpreted as remnants of
relativistic solitons (“post-solitons”)
[Borghesi et al., Phys. Rev. Lett. **88** (2002) 135002]

Ion modulations resulting from onset and evolution of
Buneman instability in the late evolution of a plasma wake
[Borghesi et al., Phys. Rev. Lett. **94** (2005) 195003]

Collisionless shock waves in the plasma blow-off
[Romagnani et al., Phys. Rev. Lett. **101** (2008) 025004]

Observation of **phase space holes**
[Sarri et al., arXiv:0908.4527]

... and other including the ones discussed in the following
(**plasma sheath expansion**, **relativistic self-channeling**,
“Hybrid” magnetic structures, **ultrafast charging** ...)

Additional applications in experiments of relevance for Inertial Confinement Fusion (radiography of implosions and shocks, detection of self-generated fields) have been demonstrated by several groups (QUB, Rutherford, LULI, Livermore, Rochester, ...)

Detection of Proton-Accelerating Sheath Fields

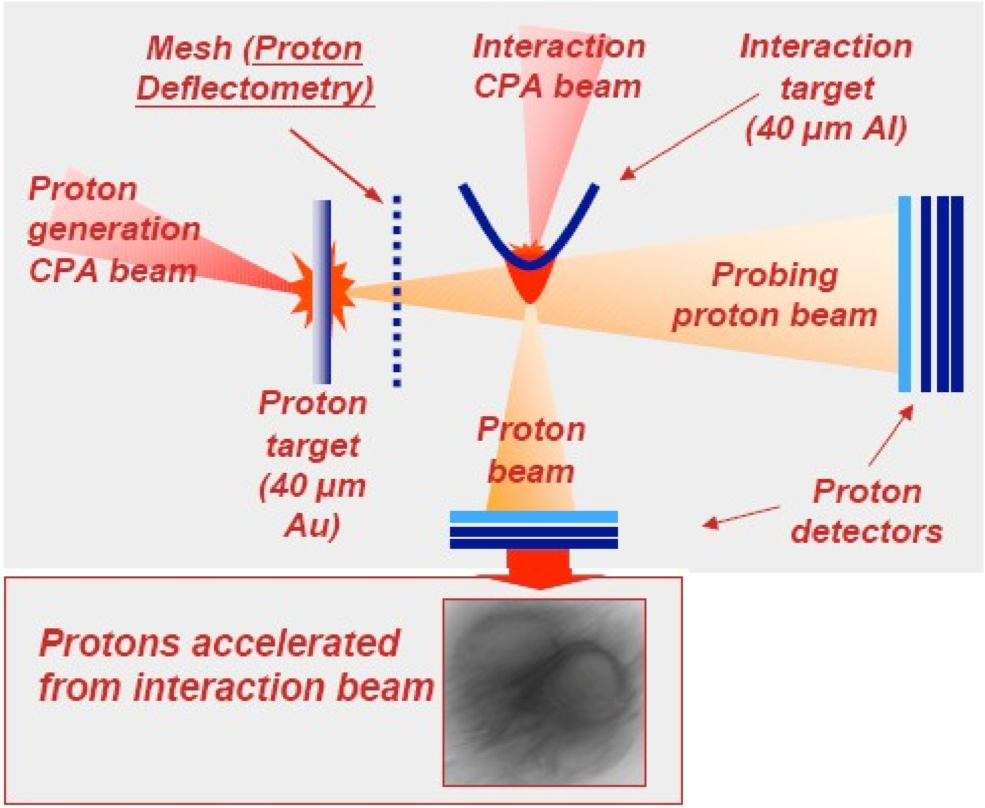

Goal: study of TNSA mechanism for ion acceleration by the direct detection of related space-charge electric field

Technique: use a second proton beam as a transverse probe

Detection of Proton-Accelerating Sheath Fields

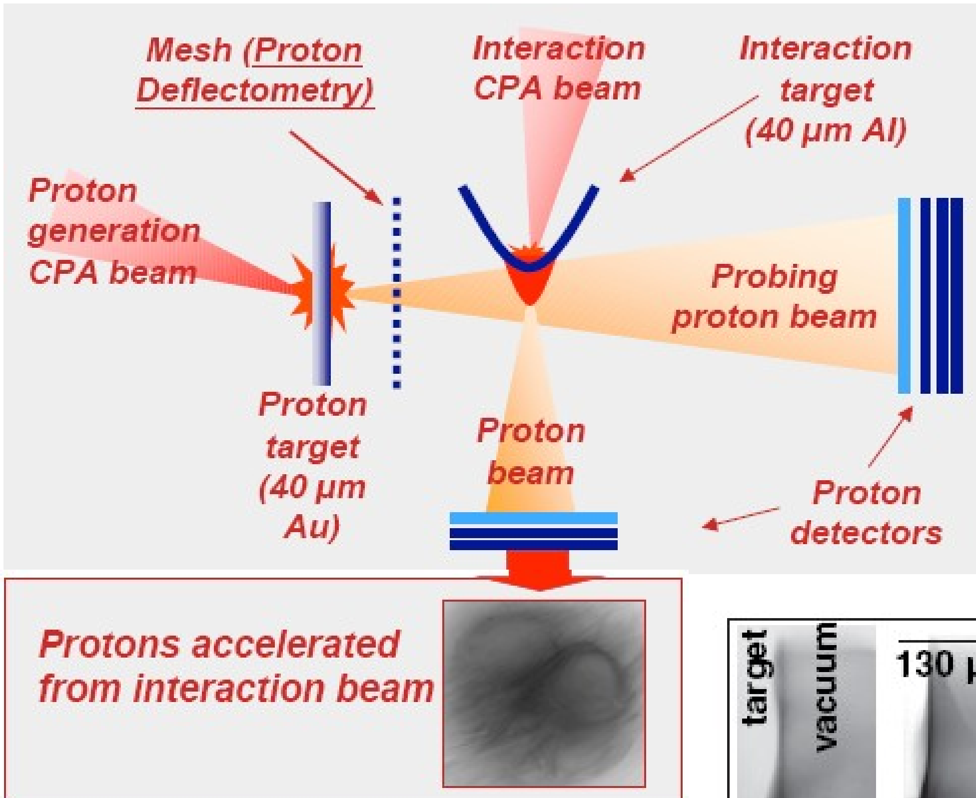

deflectometry

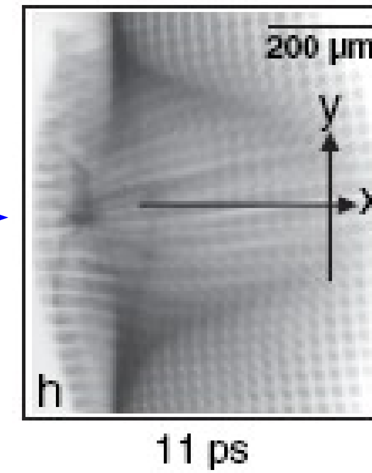

imaging

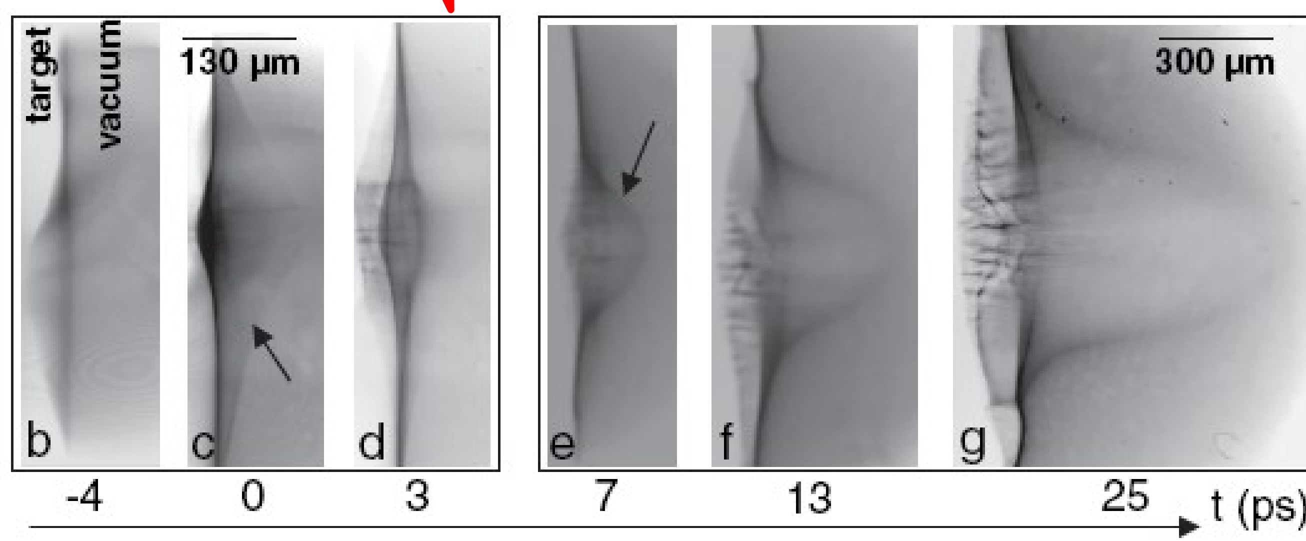

Expanding,
bell-shaped front
observed in proton
images and
deflectograms

L. Romagnani, J. Fuchs, M. Borghesi, P. Antici, P. Audebert, F. Ceccherini, T. Cowan, T. Grismayer, S. Kar, A. Macchi, P. Mora, G. Pretzler, A. Schiavi, T. Toncian, O. Willi, Phys. Rev. Lett. **95** (2005) 195001

Comparison with simulations

Experimental results have been compared with PIC simulations using the plasma expansion model (classic problem of plasma physics!)

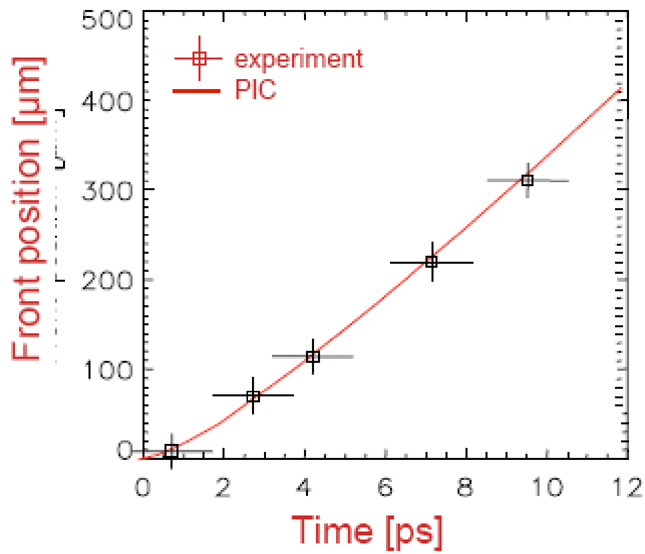

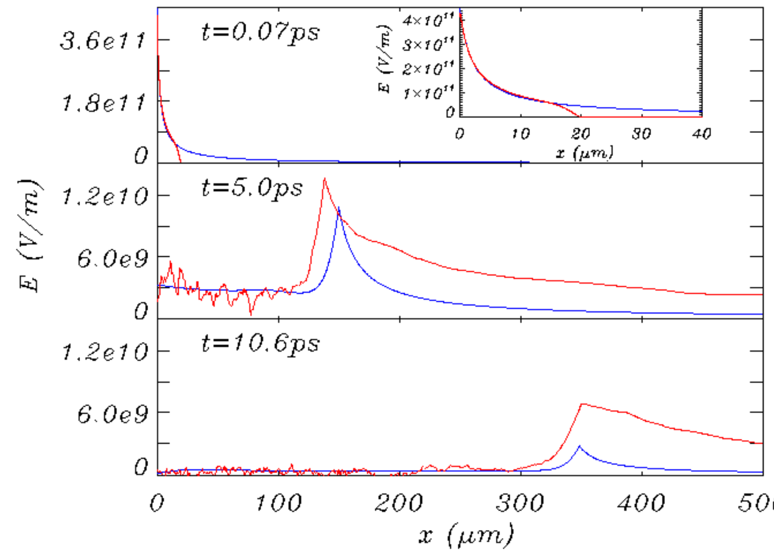

Particle tracing simulations of proton deflection in the PIC fields (plus an “heuristic” modeling of the 2D expansion) fit well experimental images and deflectrograms

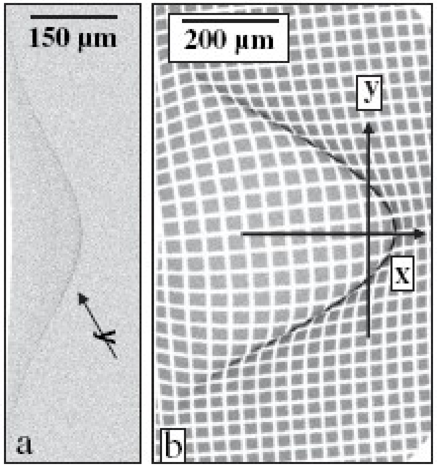

Comparison of fluid and kinetic (PIC) results show the importance of **non-**equilibrium, **kinetic** and **non-Maxwellian** effects in the plasma expansion

L. Romagnani, J. Fuchs, M. Borghesi, P. Antici, P. Audebert, F. Ceccherini, T. Cowan, T. Grismayer, S. Kar, A. Macchi, P. Mora, G. Pretzler, A. Schiavi, T. Toncian, O. Willi, Phys. Rev. Lett. **95** (2005) 195001

Study of charge-displacement self-channeling

A superintense laser pulse propagating in a low-density plasma (produced in a gas jet) undergoes self-focusing and channeling due to both relativistic effects and radial plasma expulsion by radiation pressure.

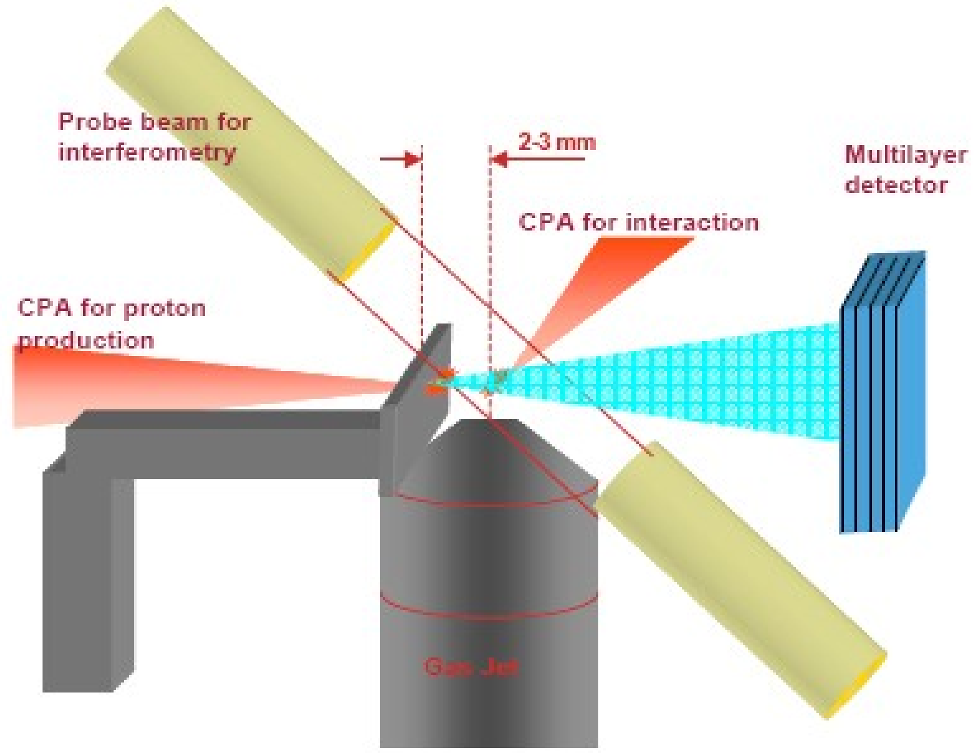

For a transient stage the channel is charged since electrons are expelled first.

Proton probing along the direction perpendicular to propagation has been used to study this effect

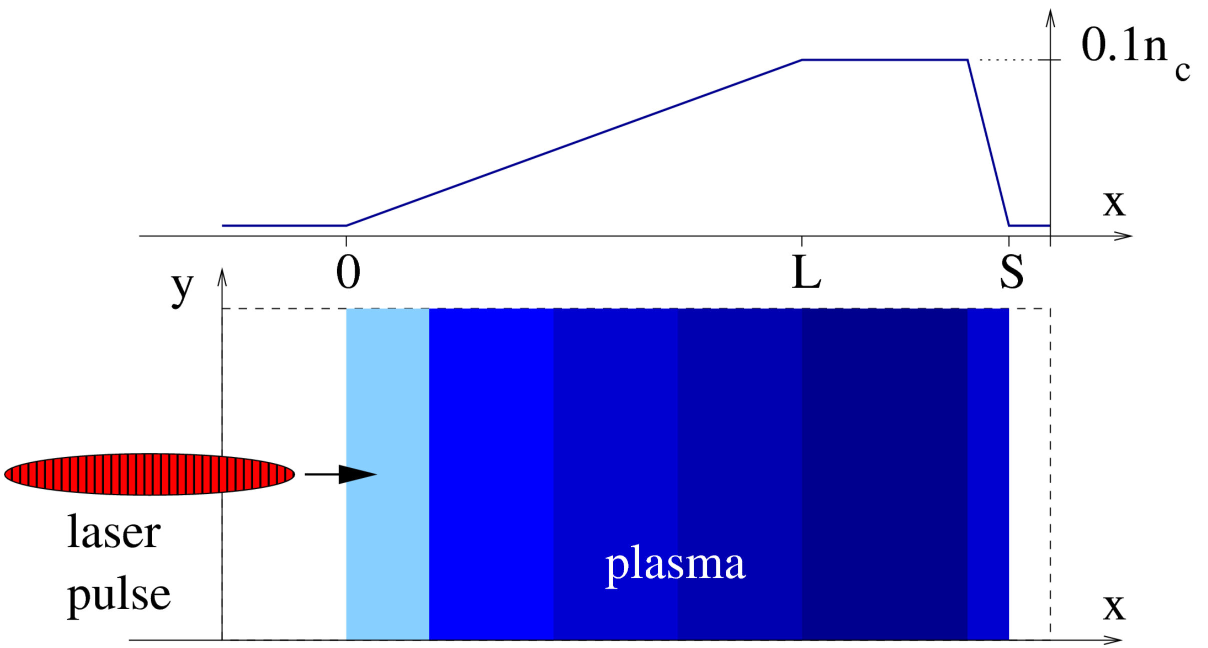

Proton images of charged channel evolution

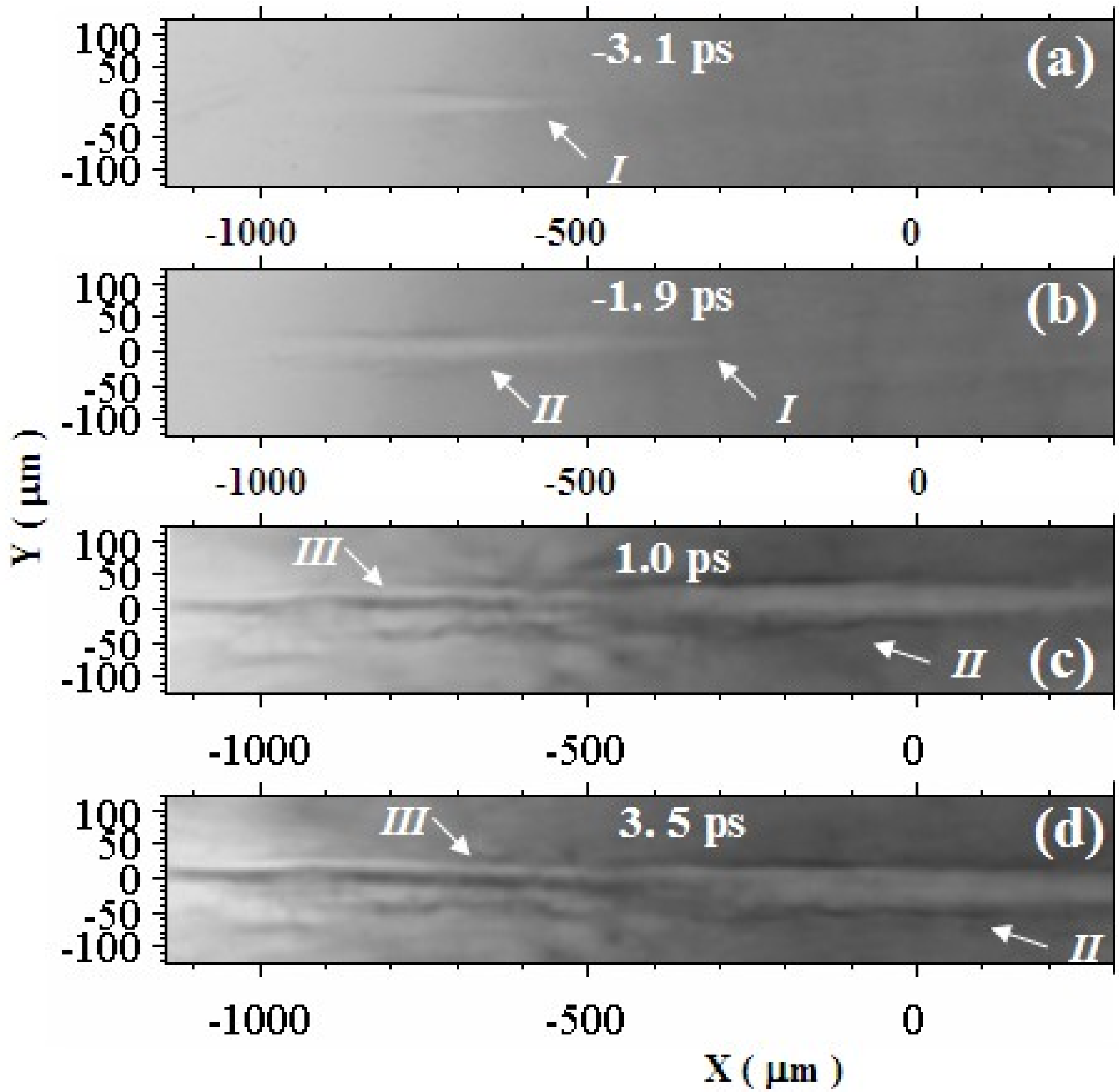

Early times (during the laser pulse) propagating "white" channel front indicates electron expulsion from the axis

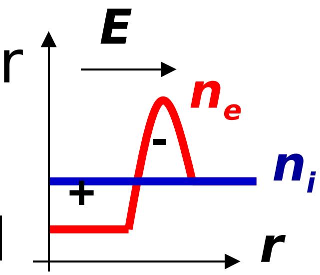

Late times (after the laser pulse) "black" line on axis indicates field inversion at some location

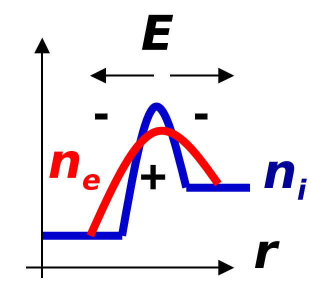

S.Kar, M.Borghesi, C.A.Cecchetti, L.Romagnani, F.Ceccherini, T.V.Lyseikina, A. Macchi, R.Jung, J.Osterholz, O.Willi, M.Galimberti, L.A.Gizzi, A.Schiavi, R.Heathcote, New J. Physics **9**, 402 (2007)

Channel front propagation speed

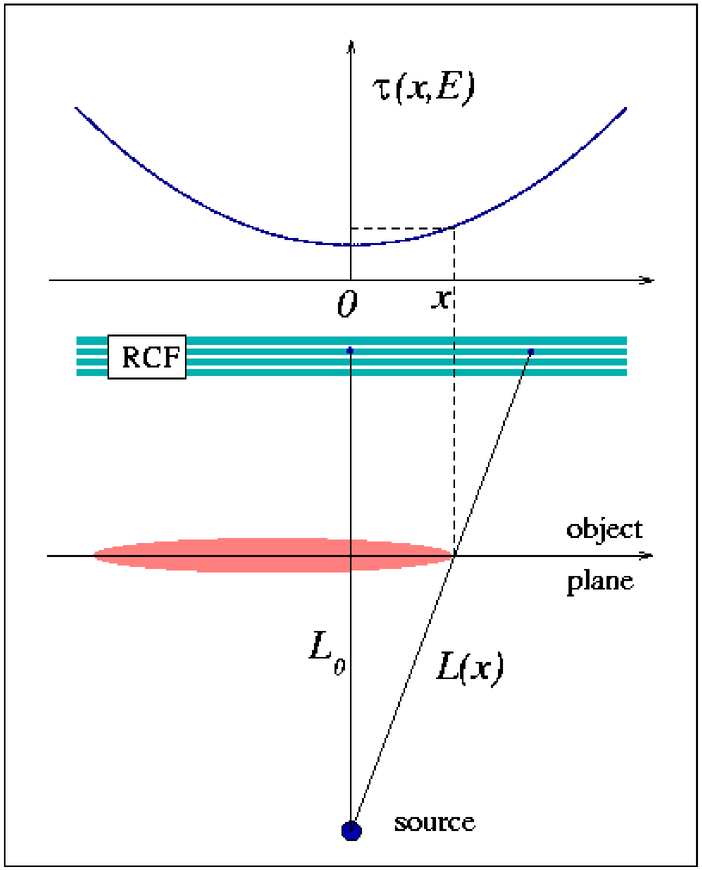

Due to the divergence of the proton beam the "probing time" depends on angle (i.e. on the position on the object plane)

$$\tau(x,E) = t_0(E) + \frac{L_0}{\sqrt{2E/m_p}}\left(\sqrt{1+x^2/L_0^2}-1\right)$$

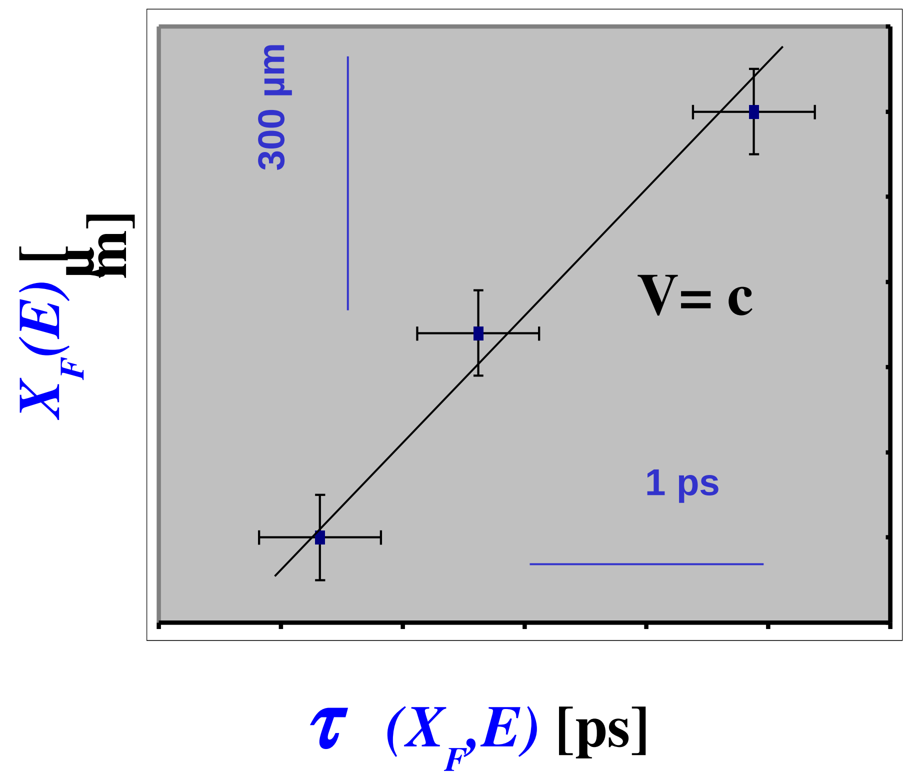

Plotting the channel front displacement $X_F(E)$ ***vs.*** the probing time τ (X_F,E) we obtain the front propagation speed $V \sim c$

2D PIC simulations show “radial” field dynamics

Laser

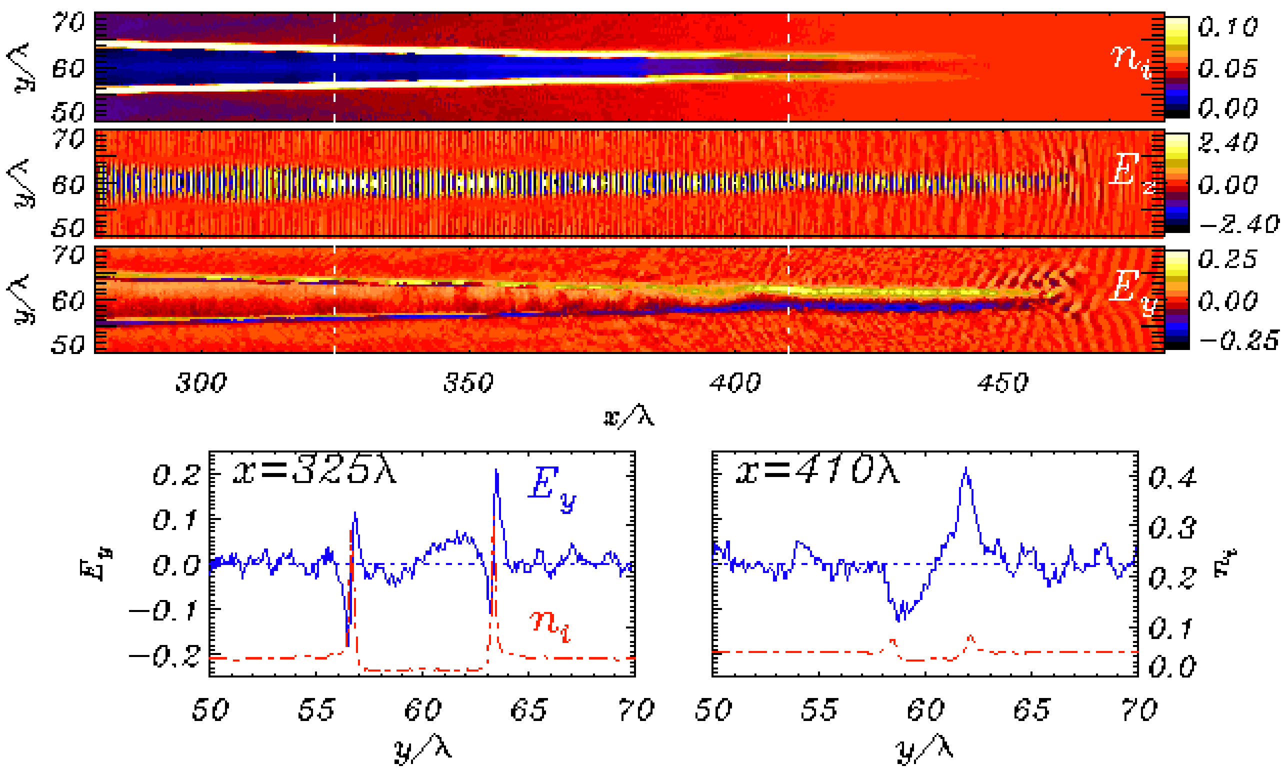

Two ambipolar fronts of E_y appear in the trailing edge of the channel; “negative” part can produce “black line” in proton images

Outward-directed radial field E_y due to electron expulsion from axis

EM component E_z reveals self-focusing

S.Kar, M.Borghesi, C.A.Cecchetti, L.Romagnani, F.Ceccherini, T.V.Lyseikina, A. Macchi, R.Jung, J.Osterholz, O.Willi, M.Galimberti, L.A.Gizzi, A.Schiavi, R.Heathcote, New J. Physics **9**, 402 (2007)

Ponderomotive model of self-channeling

Assumptions:
- cylindrical symmetry
- non-evolving laser pulse
- electrostatic approximation

Solution based on kinetic PIC model

$$
\begin{aligned}
m_e dv_e/dt &= -eE_r - m_e c^2 \partial_r \sqrt{1+a^2} \\
a = a(x,r,t) &= a_0 e^{-r^2/r_0^2 - (x-ct)^2/c^2\tau^2} \\
m_i dv_i/dt &= ZeE_r \\
\frac{1}{r}\partial_r (r \cdot E_r) &= 4\pi e (Zn_i - n_e)
\end{aligned}
$$

Particle tracing simulations using $\mathbf{E}$ from PIC model well reproduce experimental features

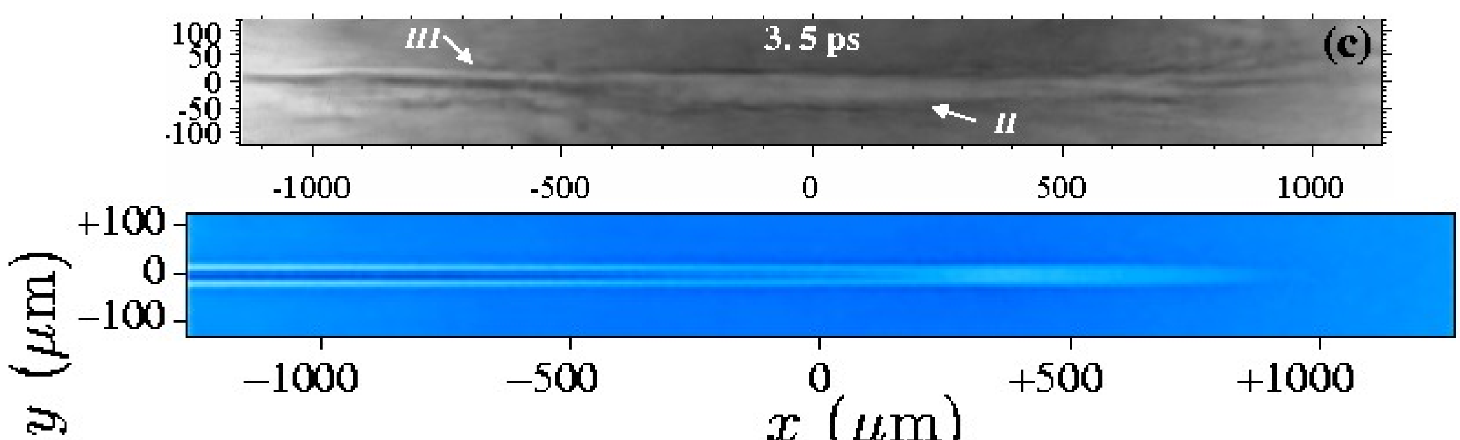

S.Kar, M.Borghesi, C.A.Cecchetti, L.Romagnani, F.Ceccherini, T.V.Lyseikina, A. Macchi, R.Jung, J.Osterholz, O.Willi, M.Galimberti, L.A.Gizzi, A.Schiavi, R.Heathcote, New J. Physics **9**, 402 (2007)

Ponderomotive model of self-channeling

Assumptions:
- cylindrical symmetry
- non-evolving laser pulse
- electrostatic approximation

Solution based on kinetic PIC model

$$
\begin{aligned}
m_e dv_e/dt &= -eE_r - m_e c^2 \partial_r \sqrt{1+a^2} \\
a = a(x,r,t) &= a_0 e^{-r^2/r_0^2 - (x-ct)^2/c^2\tau^2} \\
m_i dv_i/dt &= ZeE_r \\
\frac{1}{r}\partial_r (r \cdot E_r) &= 4\pi e(Zn_i - n_e)
\end{aligned}
$$

The late ambipolar field appears after the vanishing of the early field (“echo” effect) due to hydrodynamical breaking in the ion density profile causing strong electron heating

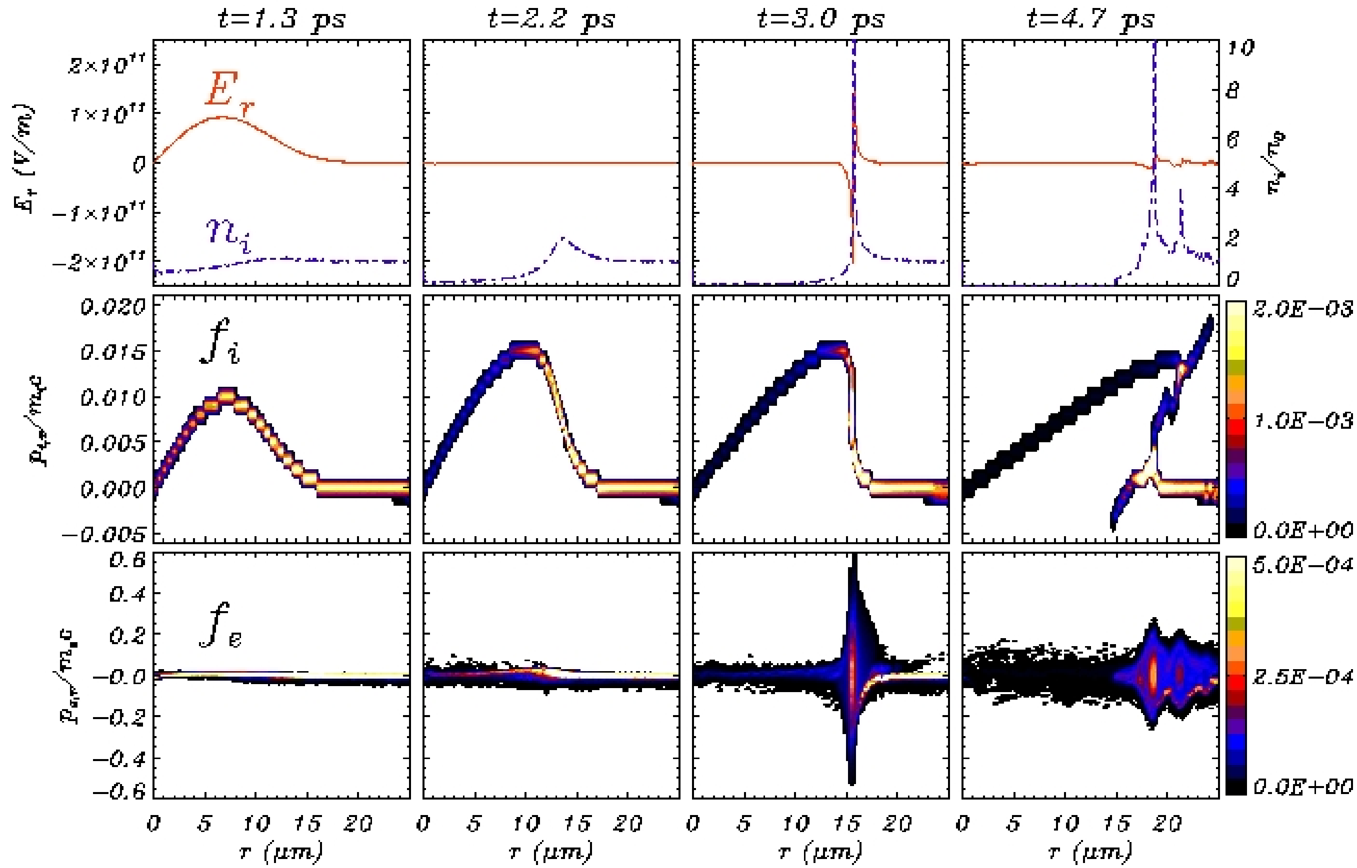

A. Macchi, F.Ceccherini, F. Cornolti, S.Kar, M.Borghesi, PPCF **51** (2009) 024005

Coherent field structures in 2D PIC simulation

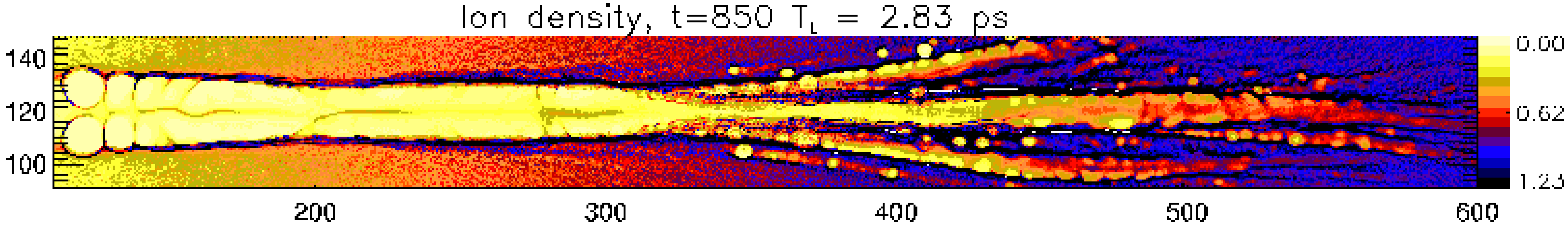

Pulse front: beam breakup
and EM **cavitons**

Left channel side:
"hybrid" quasi-periodic structures,
"part **soliton**,
part **vortex**"...

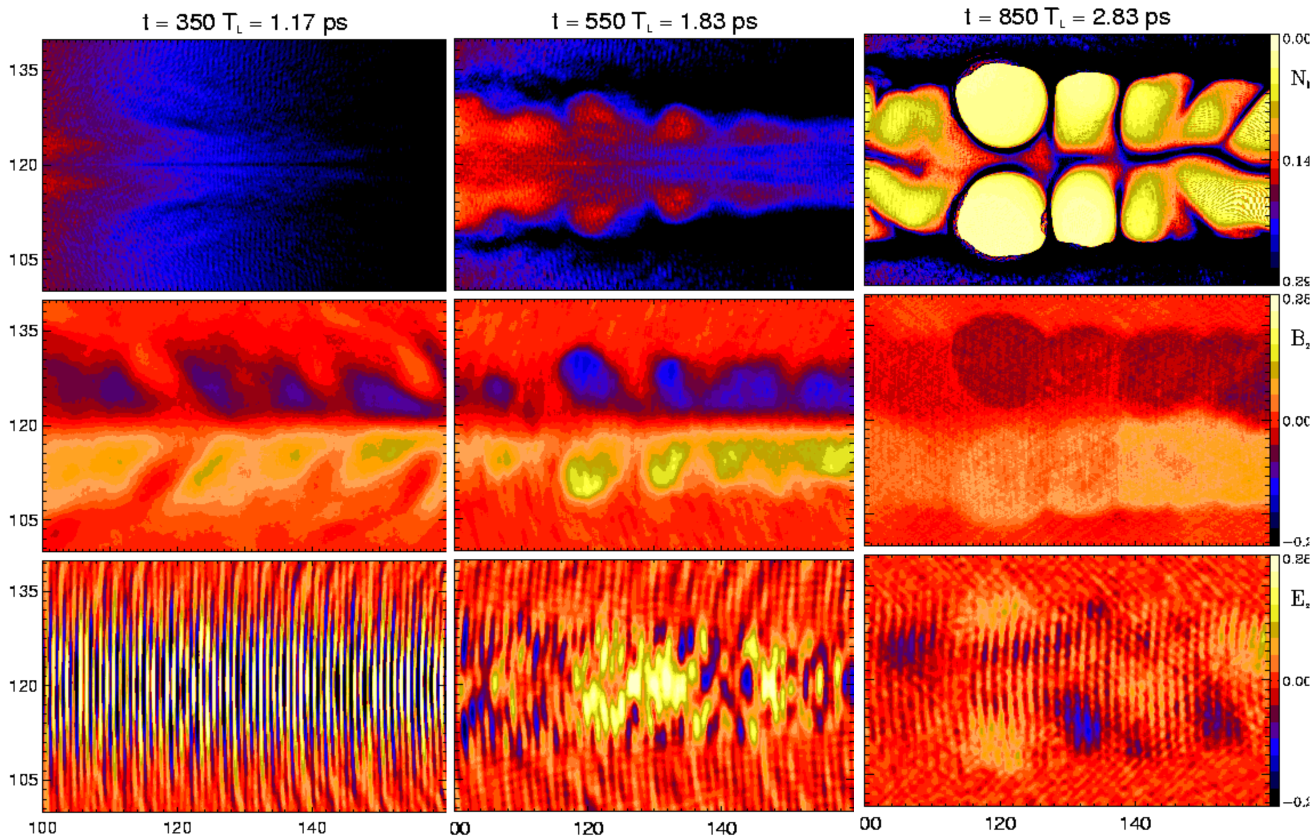

Lyseikina et al,
arXiv:physics/0701139

Macchi et al,
PPCF **49** (2007) B71

Romagnani et al,
in preparation

Simulation of proton images data: magnetic vortices?

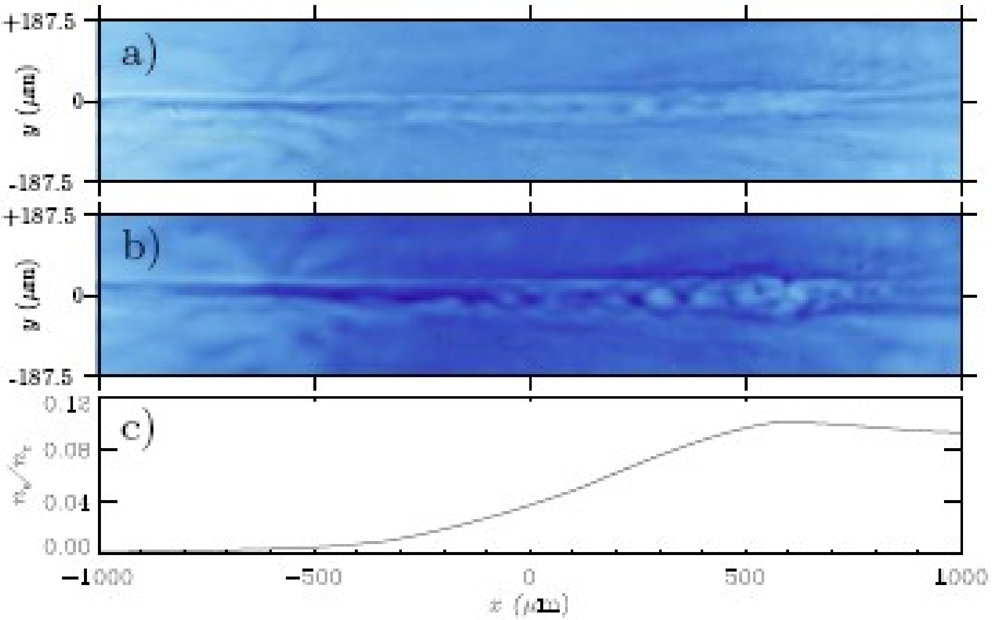

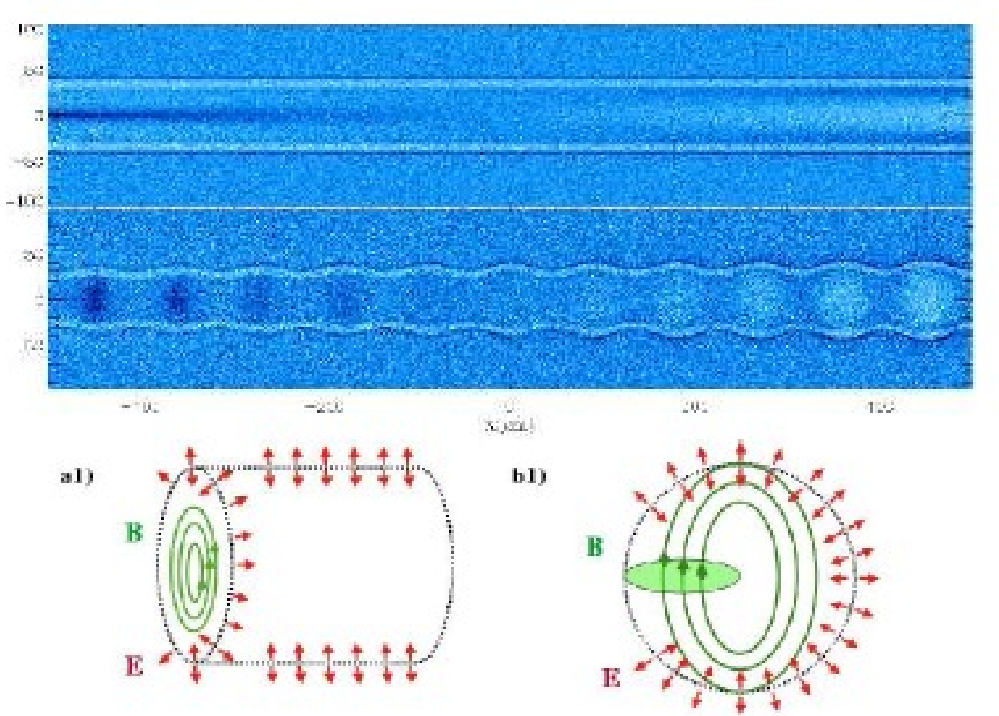

The 3D topology of the "coherent", slowly evolving structures was inferred heuristically from 2D PIC simulations and used as an input for the particle tracing code producing synthetic proton images.

The comparison suggests that image formation is dominated by magnetic field deflections and suggests the formation of patterns of "magnetized vortex rings" along the channel

Romagnani et al, in preparation

Dynamic control of proton beam properties

Concept: achieve **focusing** and **energy selection** of the proton beam by “external” devices or by “target engineering”

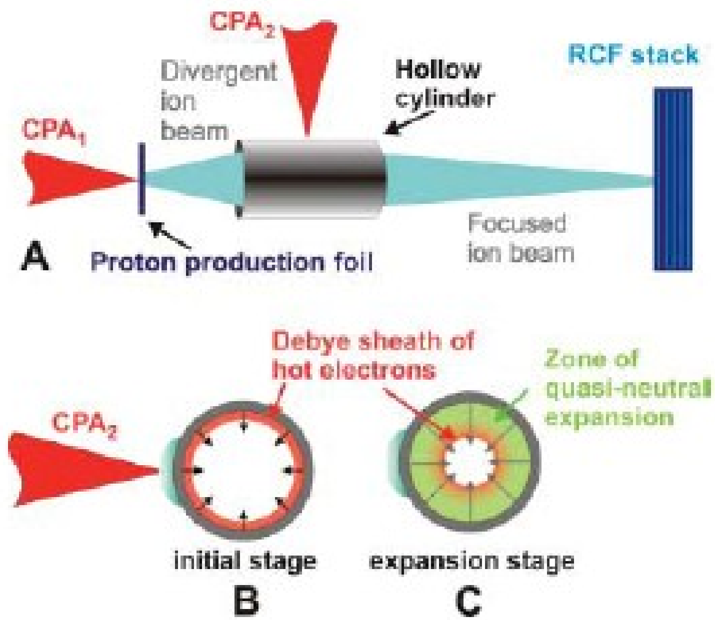

Laser-driven cylindrical microlens
Toncian et al., Science **312** (2006) 410

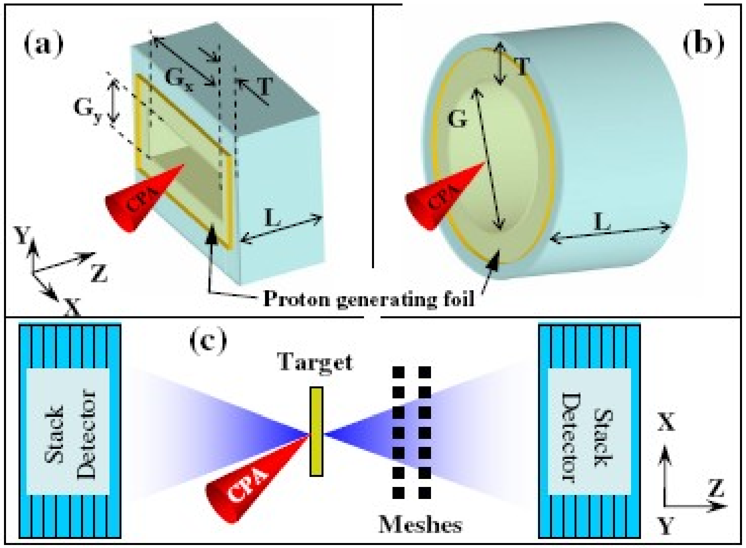

Shaped targets designed as **electrostatic (?) lenses**
Kar et al., PRL **100** (2008) 105004

Both approaches pose the question on **how rapidly** the electric field created by escaping electrons propagates on the surface of the target

Field propagation on the rear surface of solid targets

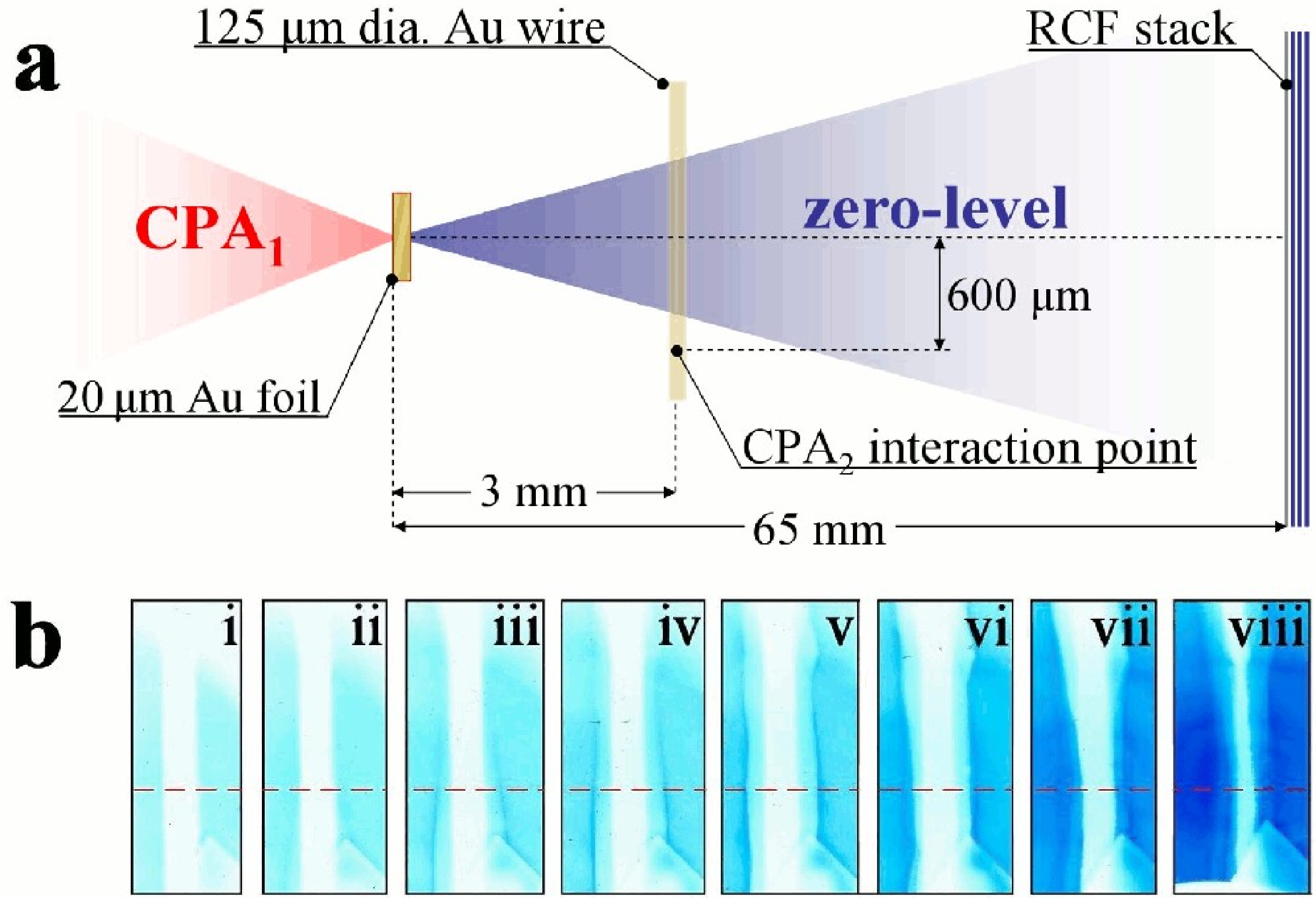

- In the interaction with a wire target a fast positive charging followed by later discharging is observed: escape of fast electrons and return neutralizing current?
- The propagation of the field out of the interaction region is not resolved with a “vertical” wire

Field propagation on the rear surface of solid targets

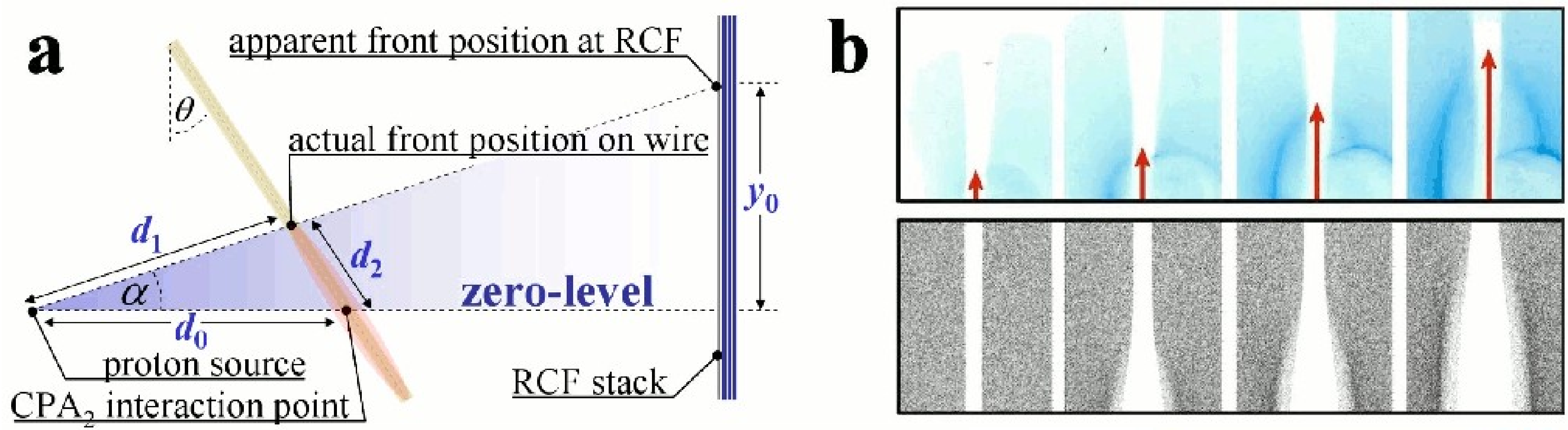

By inclining the wire to an angle θ
with respect to the vertical axis
the propagation of the field is resolved now ;

the speed v_f=0.96±0.04c

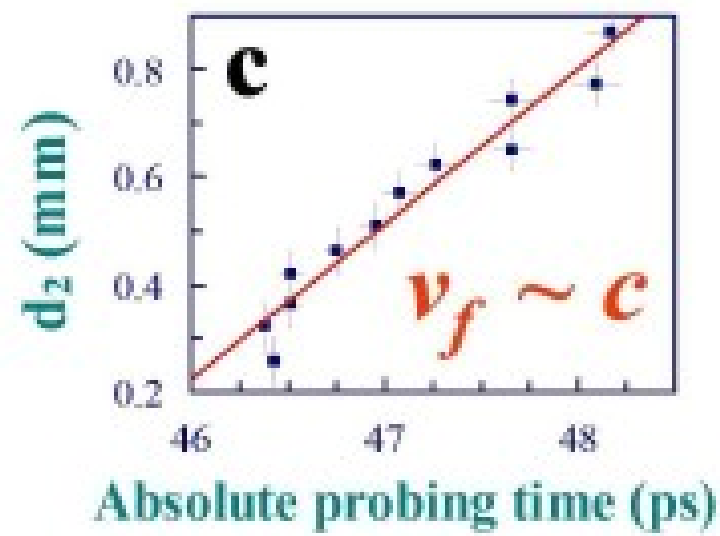

K.E.Quinn, P.A.Wilson, C.A.Cecchetti, B.Ramakrishna, L.Romagnani, G.Sarri, L. Lancia, J. Fuchs, A. Pipahl, T. Toncian, O.Willi, R.J.Clarke, D.Neely, M.Notley, P.Gallegos, D.C.Carroll, M.N.Quinn, X.H.Yuan, P.McKenna, T. V. Liseykina, A. Macchi, M. Borghesi,
PRL 102, 194801 (2009)

Flowing current and loss of electrons from the wire

From the measurement of the radial field E_r and the propagation velocity v_f it is possible to reconstruct the history of the total current I flowing trough the wire

$$J(t) = \frac{1}{2} r_{\mathrm{w}} v_f E_s(t)$$

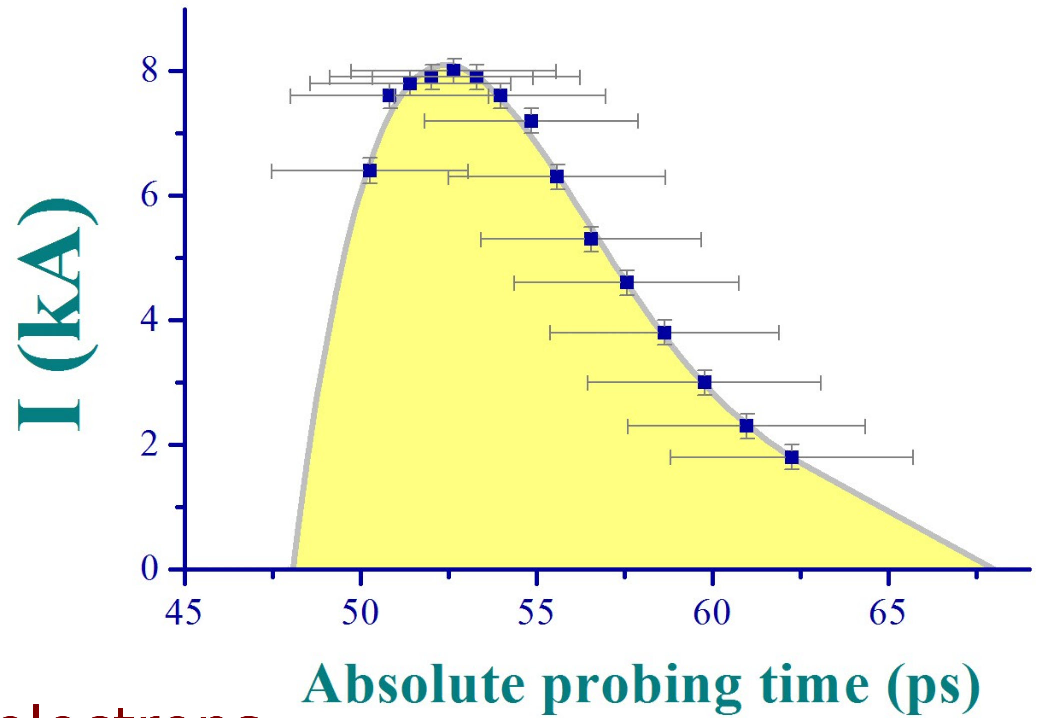

The estimate of the fraction of electrons escaped in vacuum f_{esc} thus obtained is roughly consistent with a simple estimate based on the charging of an “hot” plasma sphere or radius r_0 with N_e electrons in Boltzmann equilibrium

$$\frac{\ln f_{\mathrm{esc}}}{f_{\mathrm{esc}}} = -\frac{r_c}{r_0} \frac{m_e c^2}{k_B T_e} N_e$$

K.E.Quinn, P.A.Wilson, C.A.Cecchetti, B.Ramakrishna, L.Romagnani, G.Sarri, L. Lancia, J. Fuchs, A. Pipahl, T. Toncian, O.Willi, R.J.Clarke, D.Neely, M.Notley, P.Gallegos, D.C.Carroll, M.N.Quinn, X.H.Yuan, P.McKenna, T. V. Liseykina, A. Macchi, M. Borghesi,
PRL 102, 194801 (2009)

Simulation of field propagation on the rear surface

PIC simulations of a “model problem” show a “double front” structure of the current at the rear surface:

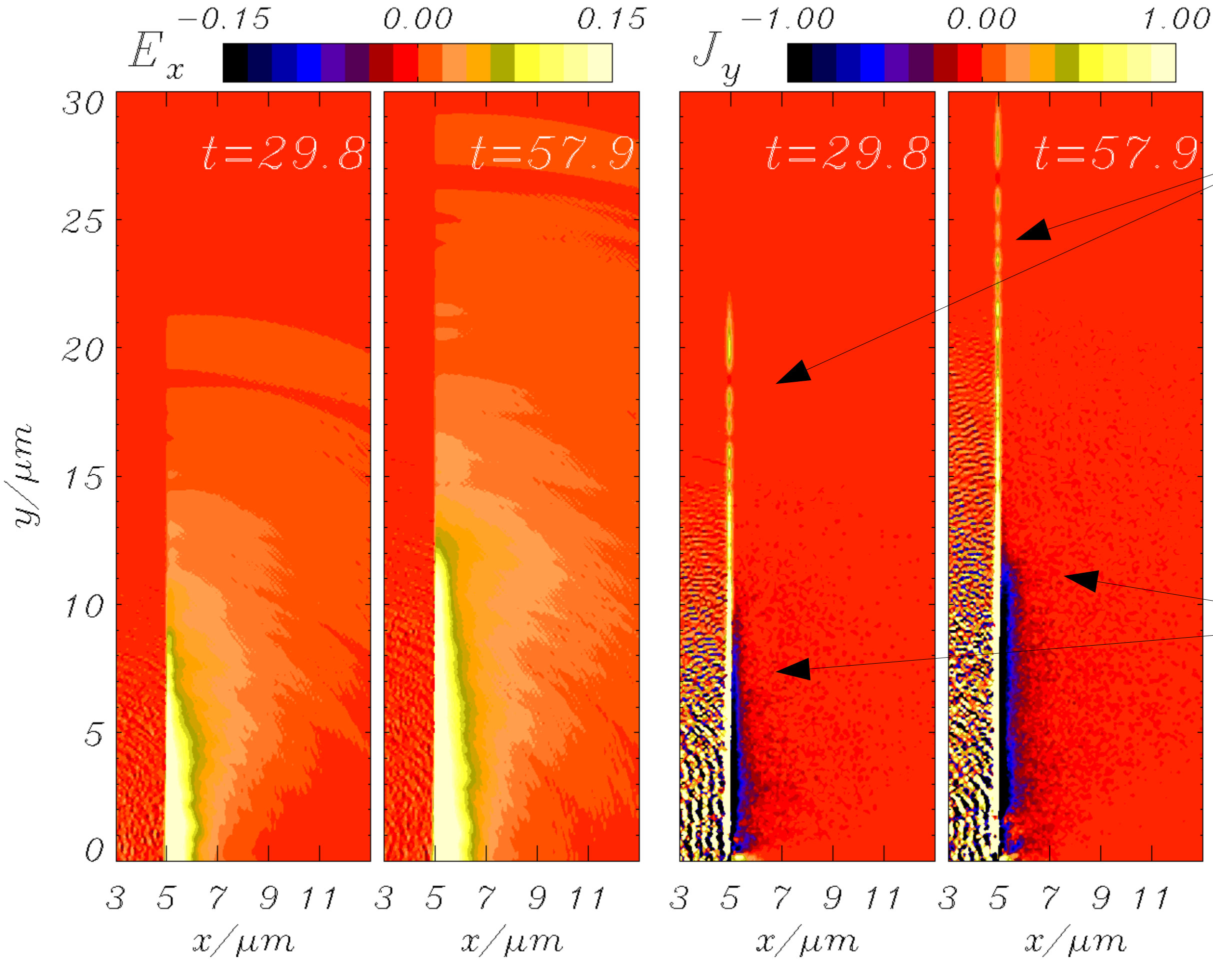

- thin current layer on the surface, propagating at speed c
-> driven by EM fields by the transient “antenna” created by escaping electrons

- bulk current of “fast” electrons, propagating slower than c
-> due to the spread of “fast” electrons in the transverse direction

K.E.Quinn, P.A.Wilson, C.A.Cecchetti, B.Ramakrishna, L.Romagnani, G.Sarri, L. Lancia, J. Fuchs, A. Pipahl, T. Toncian, O.Willi, R.J.Clarke, D.Neely, M.Notley, P.Gallegos, D.C.Carroll, M.N.Quinn, X.H.Yuan, P.McKenna, T. V. Liseykina, A. Macchi, M. Borghesi,
PRL 102, 194801 (2009)

Field propagation on the rear surface of solid targets

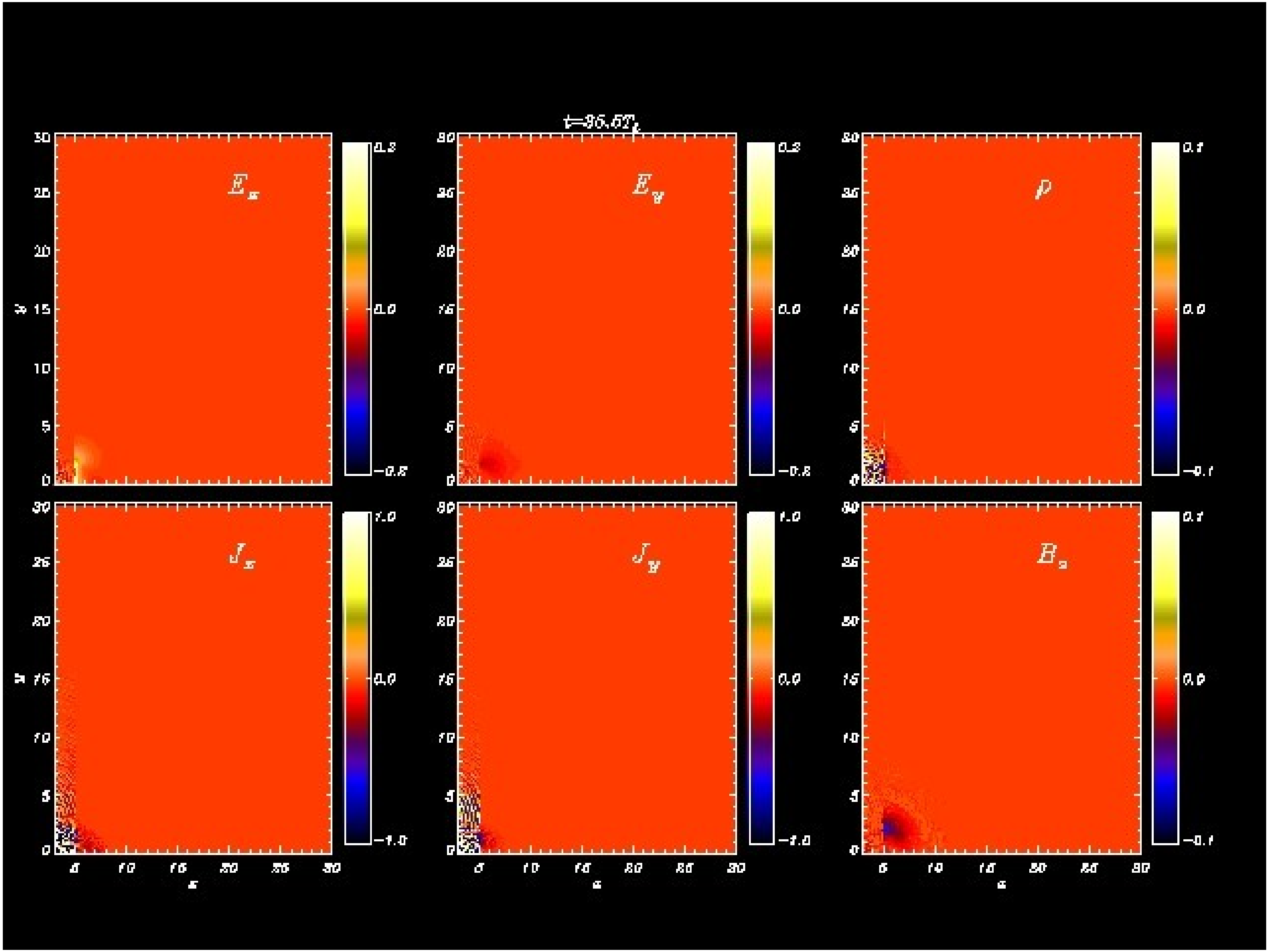

Field propagation on the rear surface of solid targets

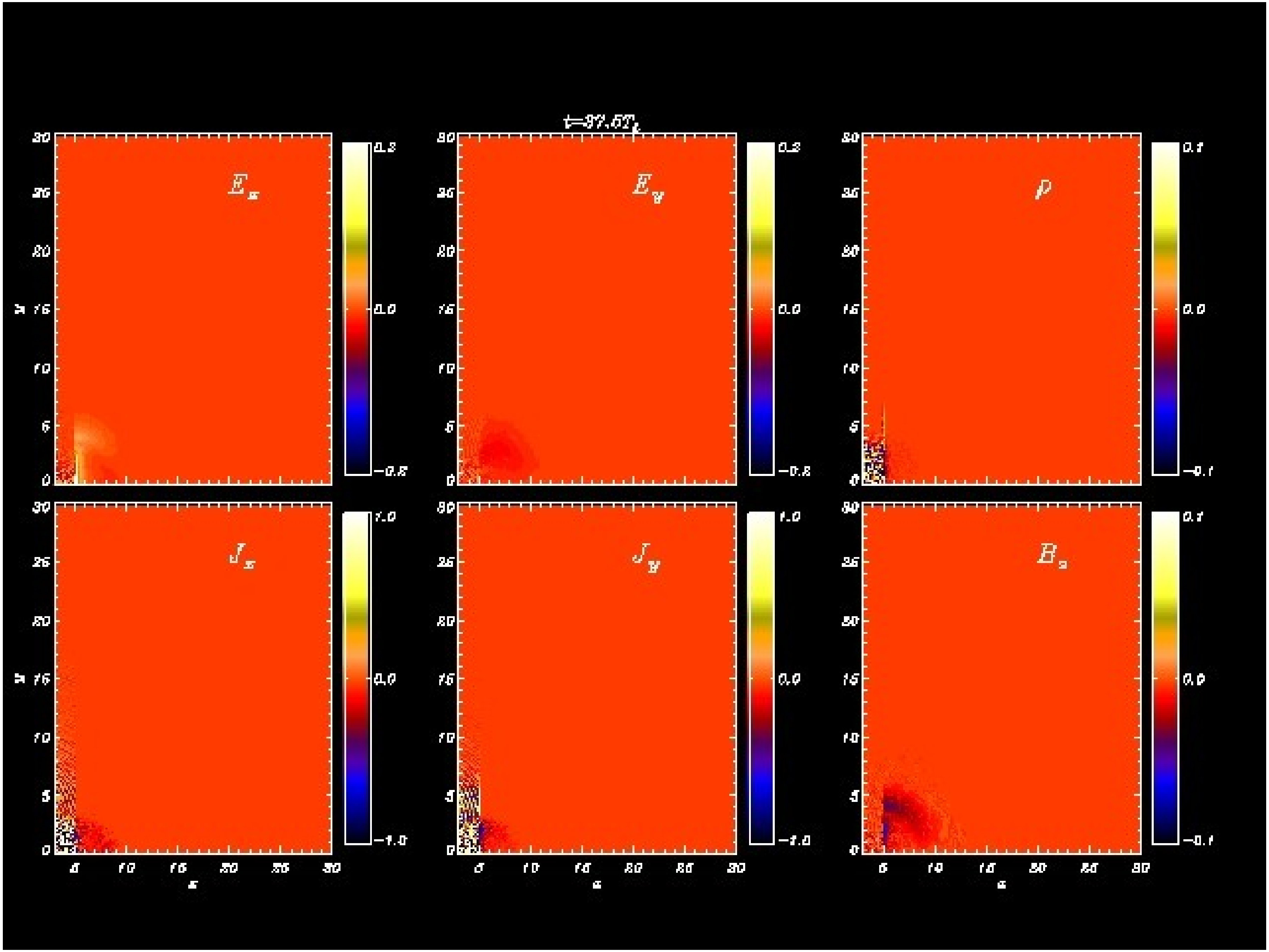

Field propagation on the rear surface of solid targets

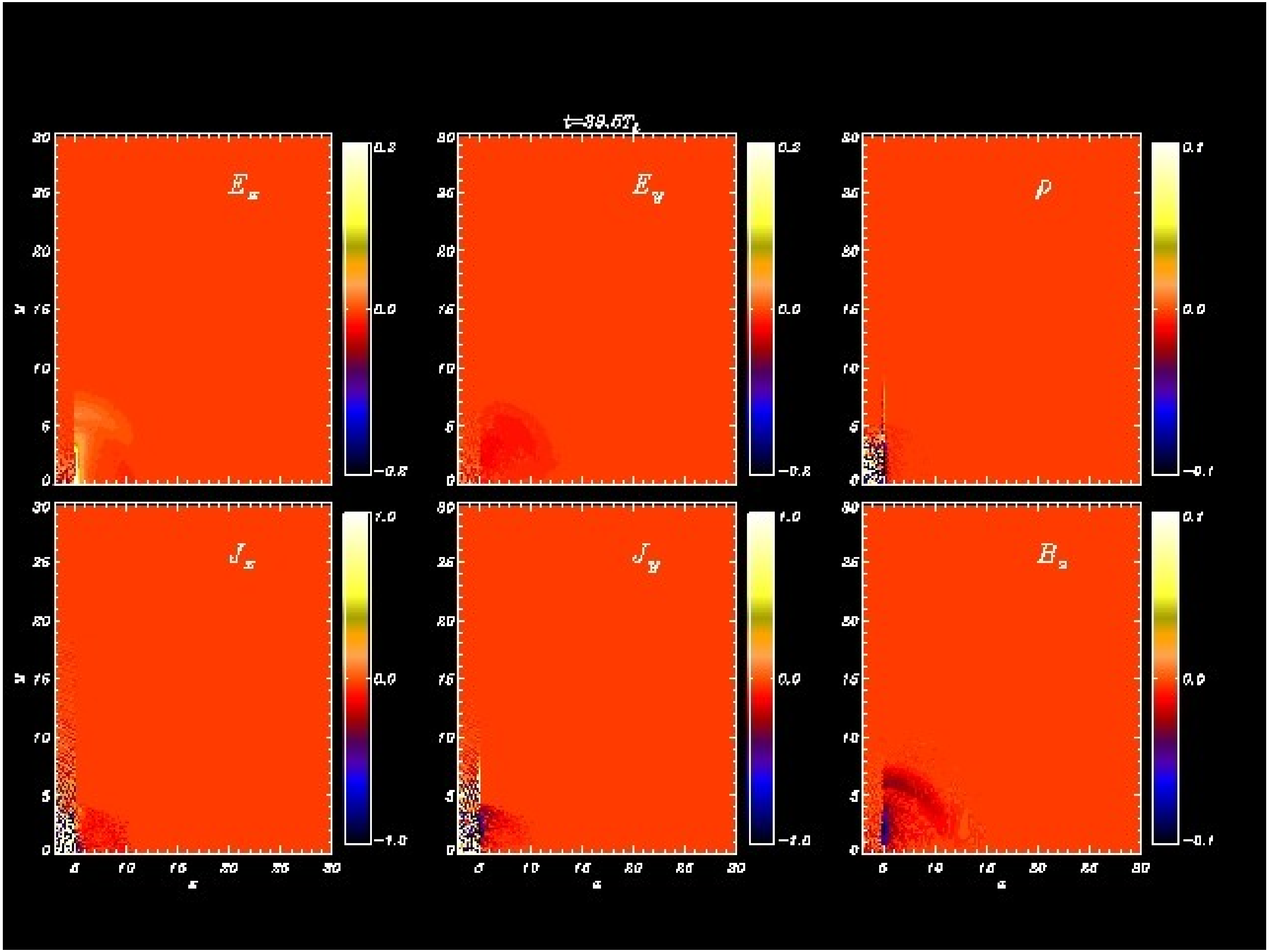

Field propagation on the rear surface of solid targets

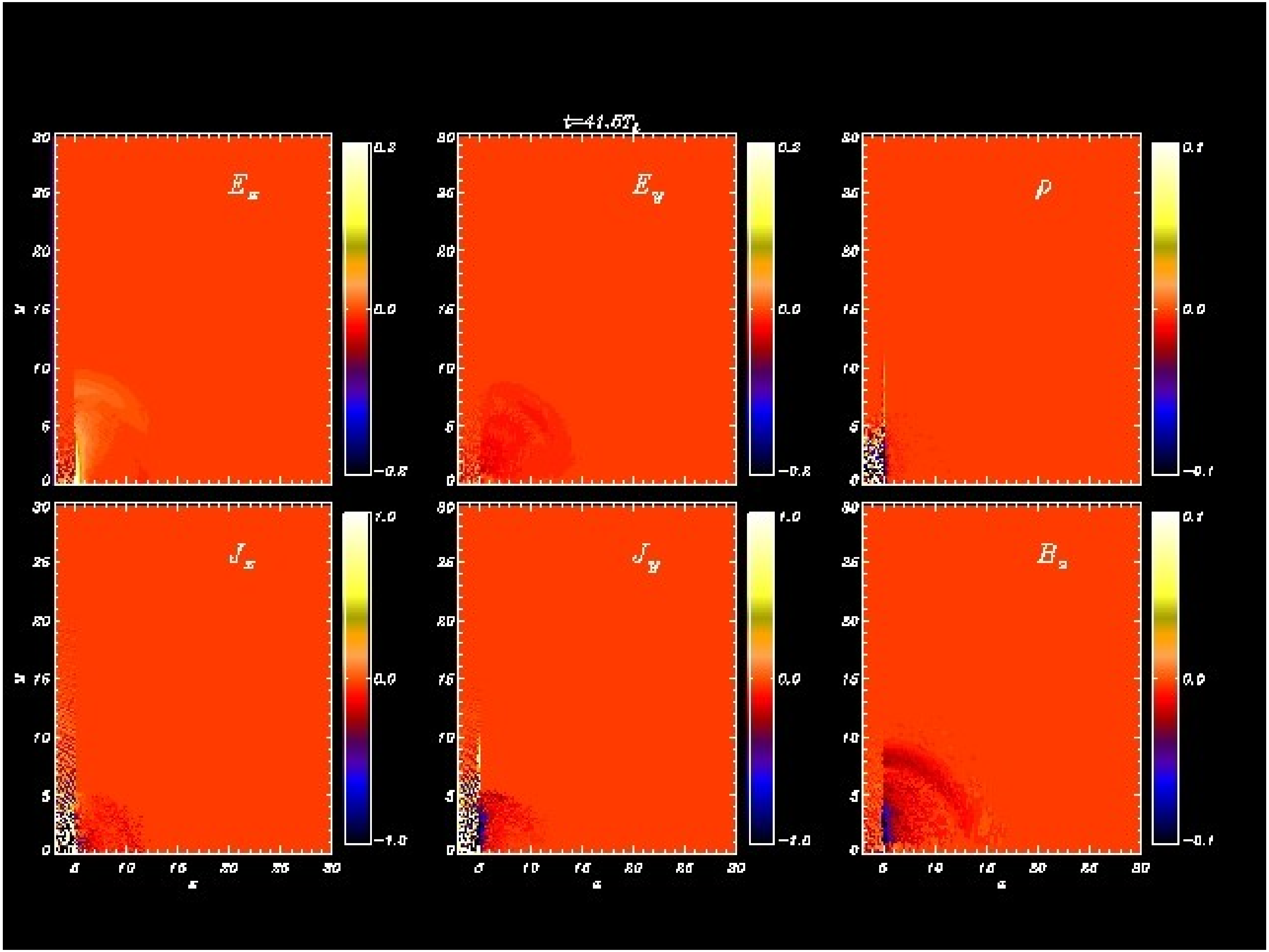

Field propagation on the rear surface of solid targets

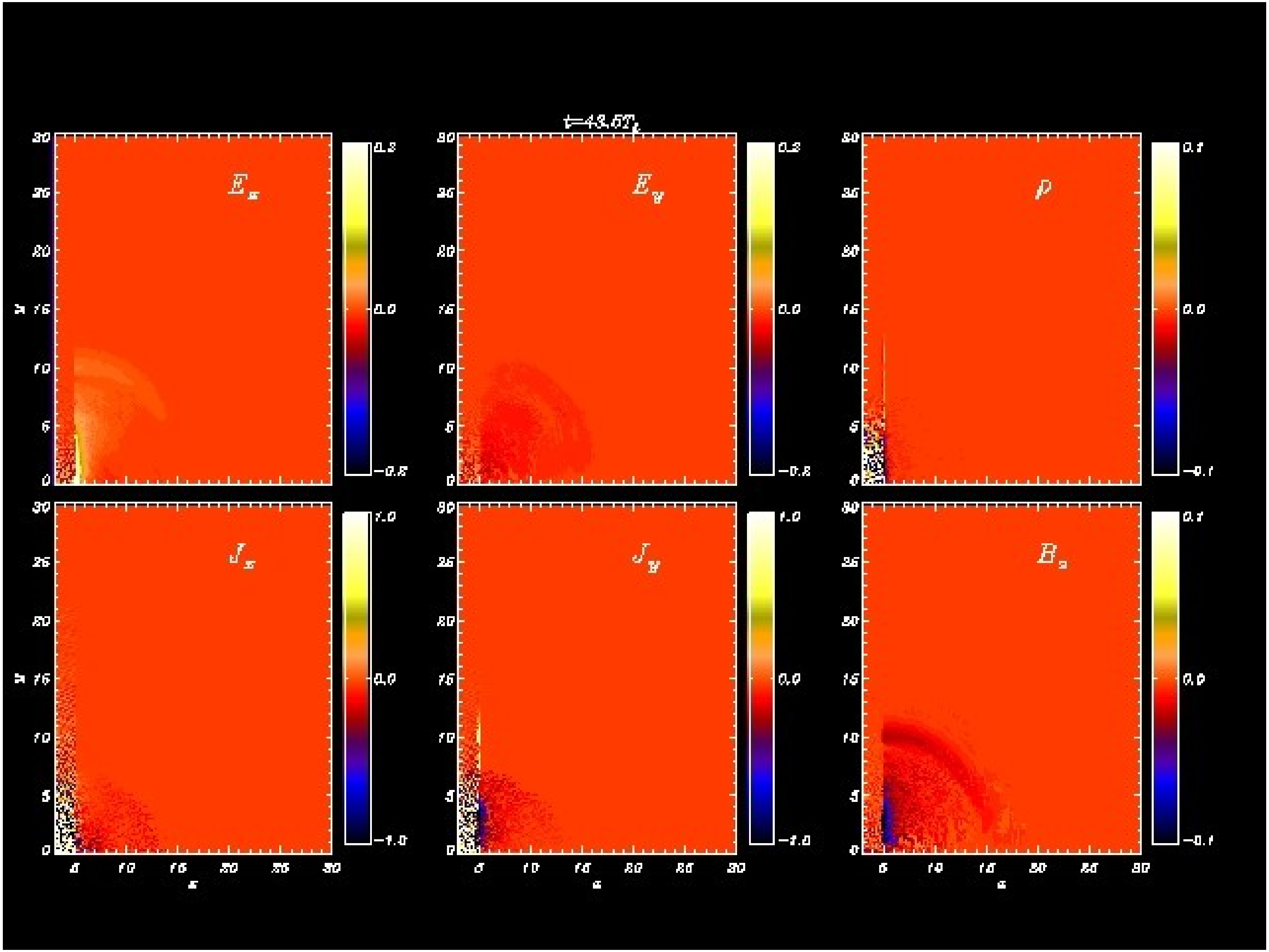

Field propagation on the rear surface of solid targets

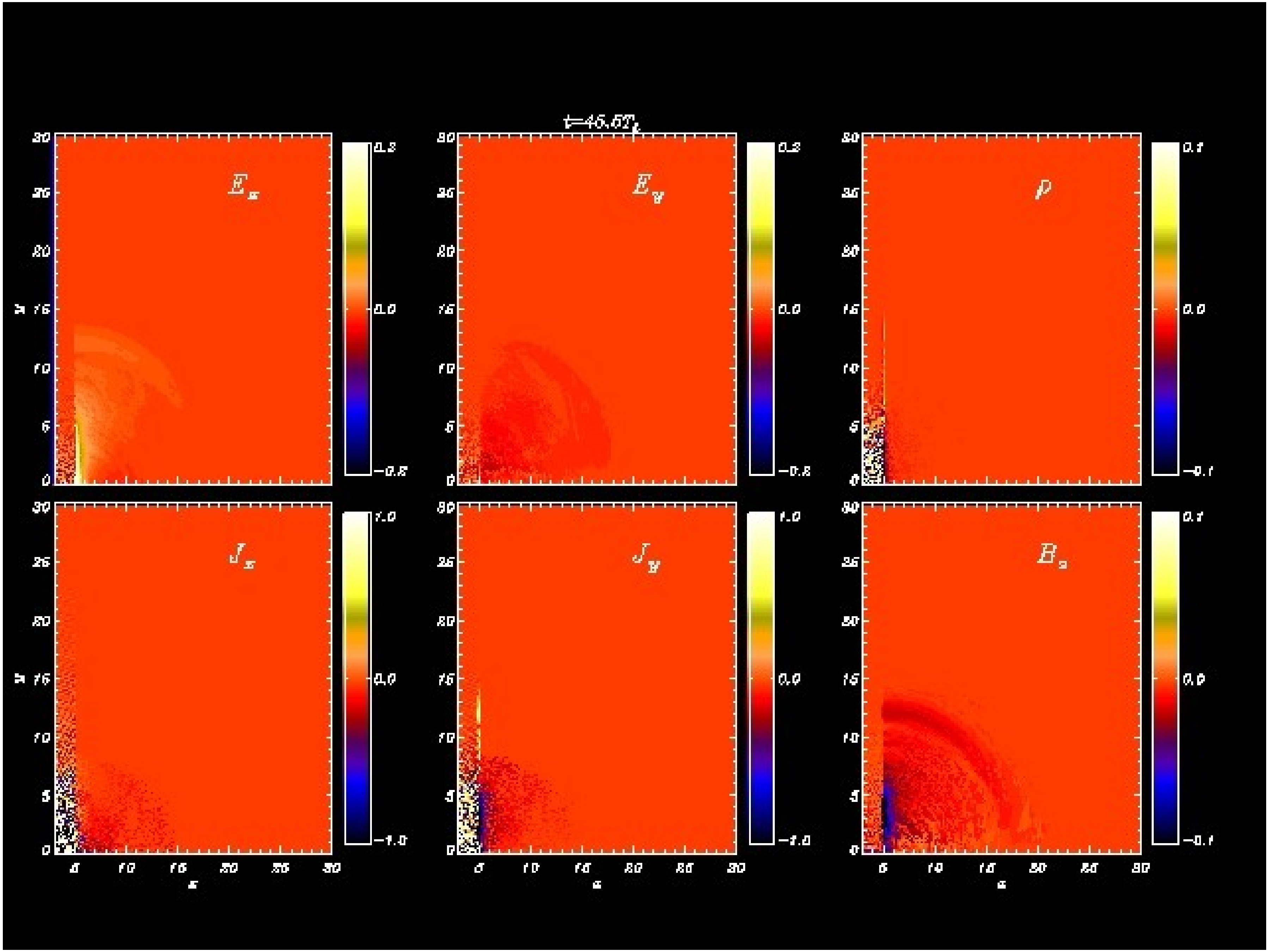

Field propagation on the rear surface of solid targets

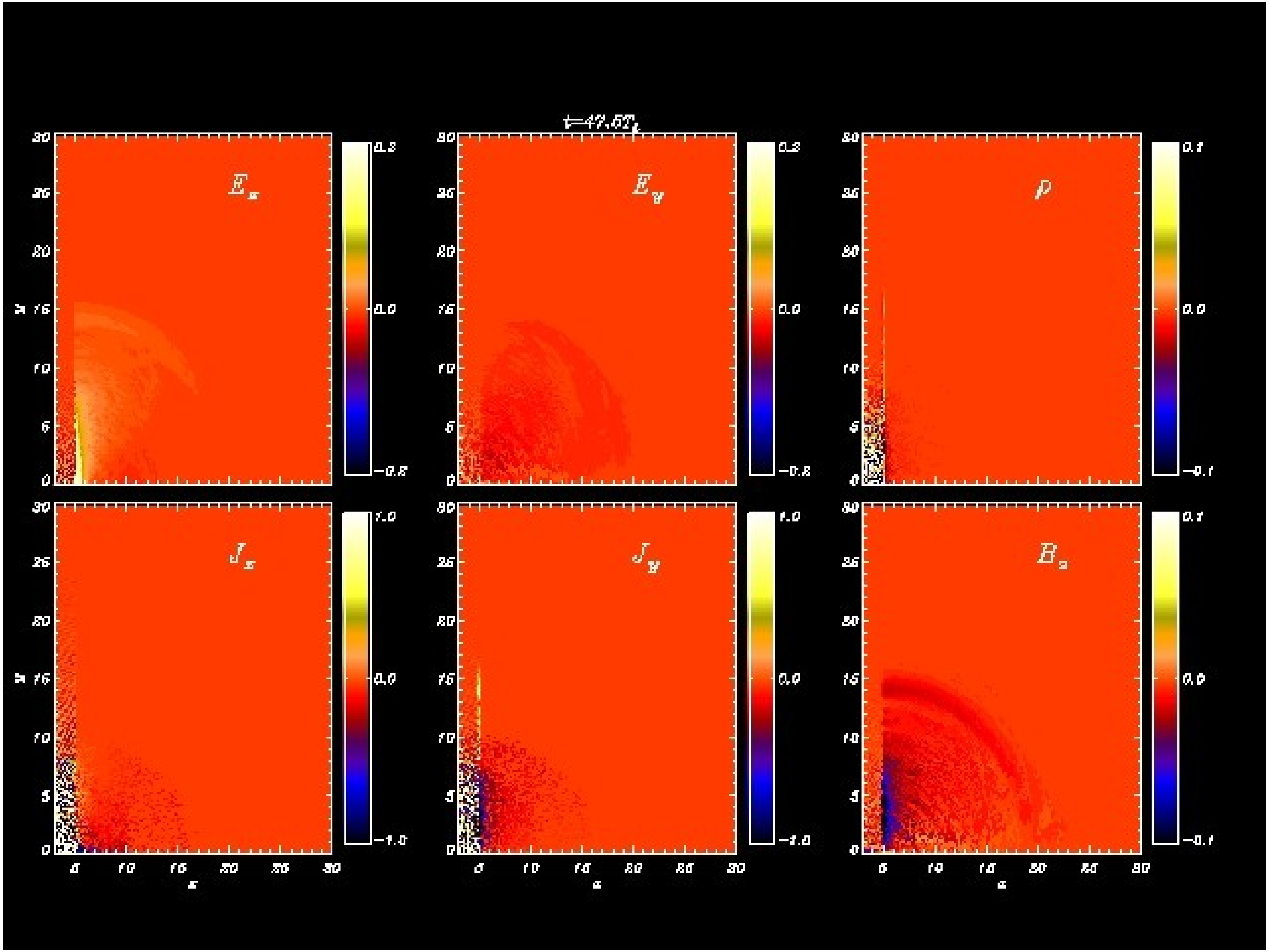

Field propagation on the rear surface of solid targets

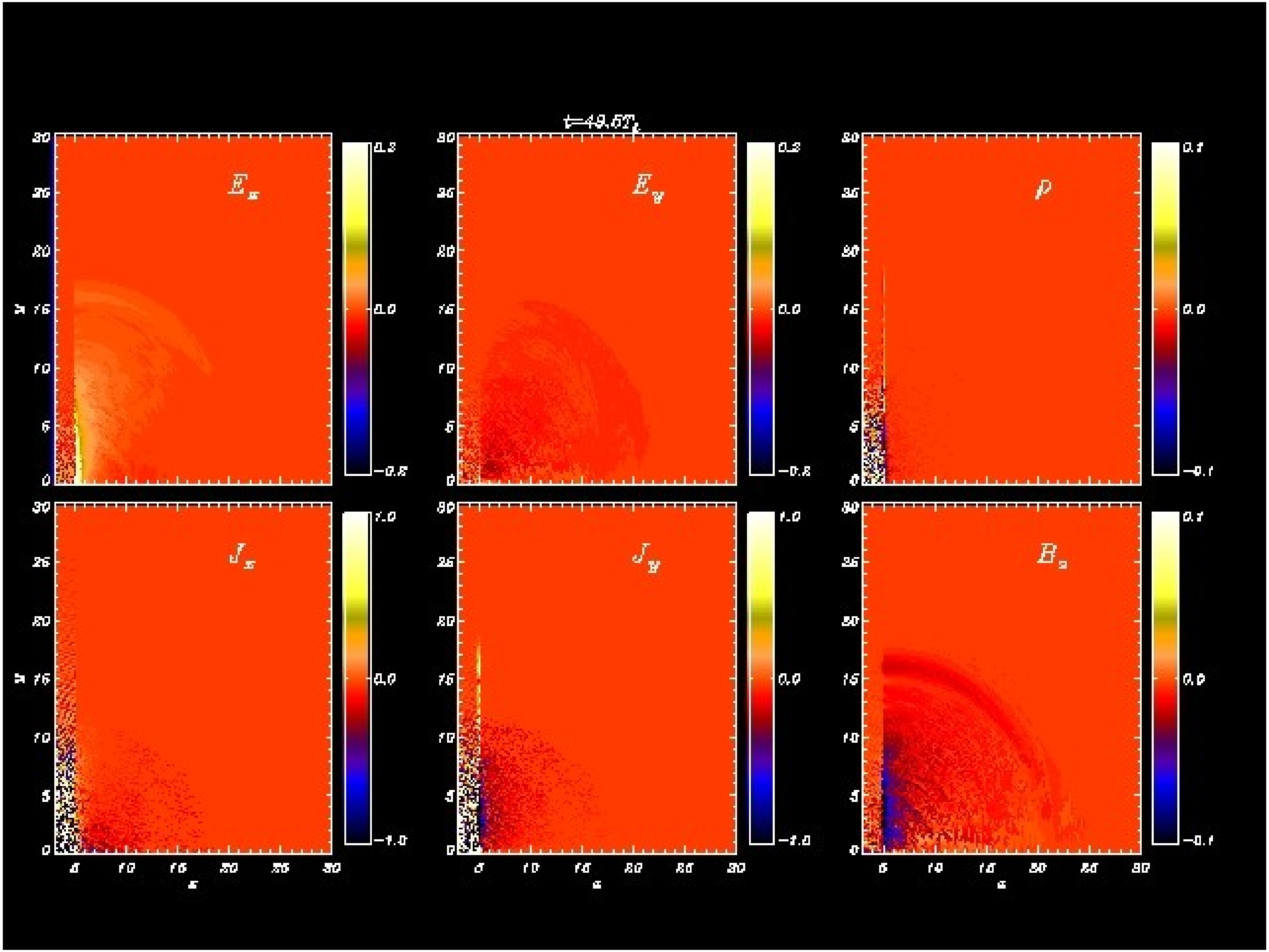

Field propagation on the rear surface of solid targets

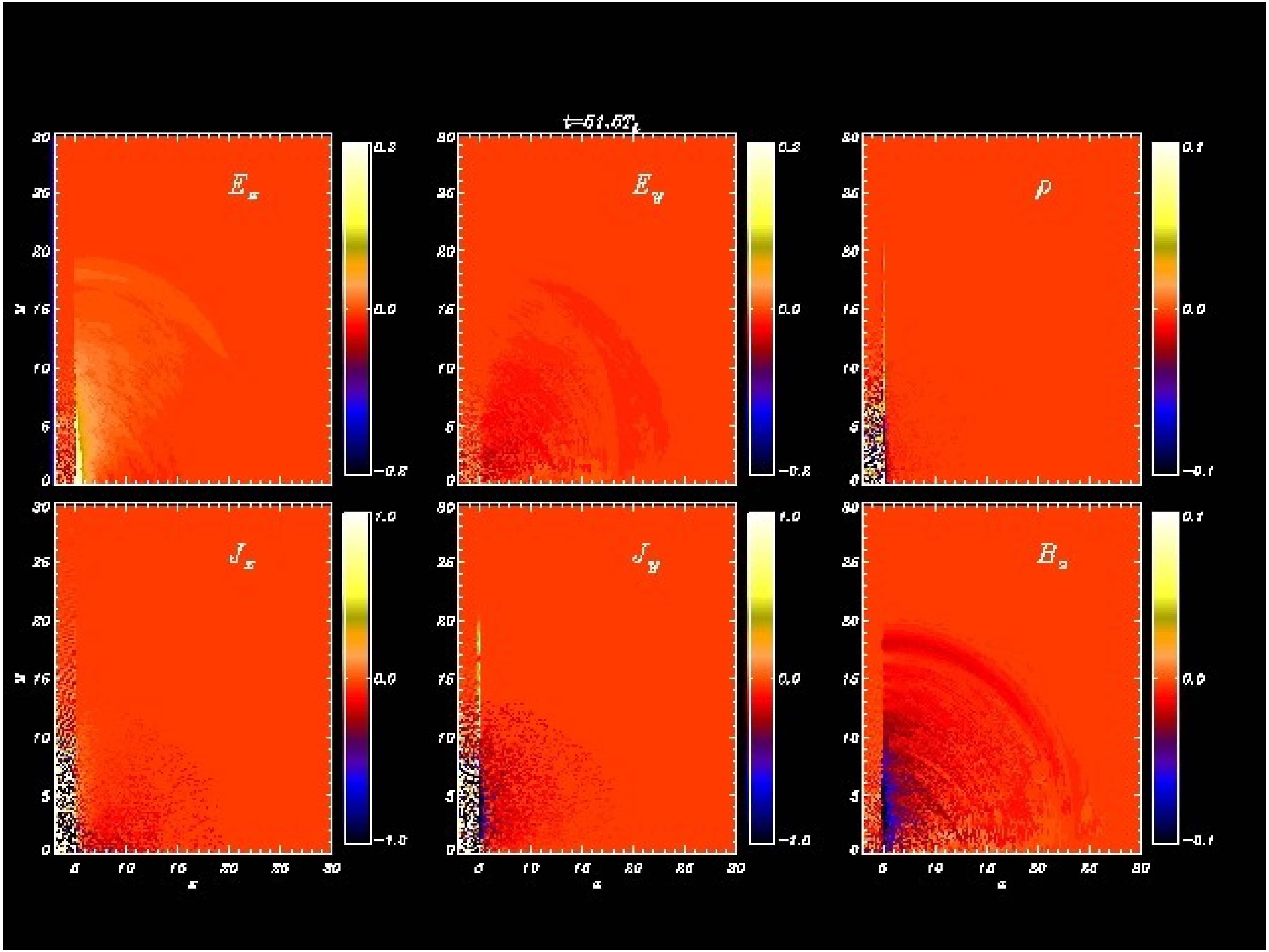

Field propagation on the rear surface of solid targets

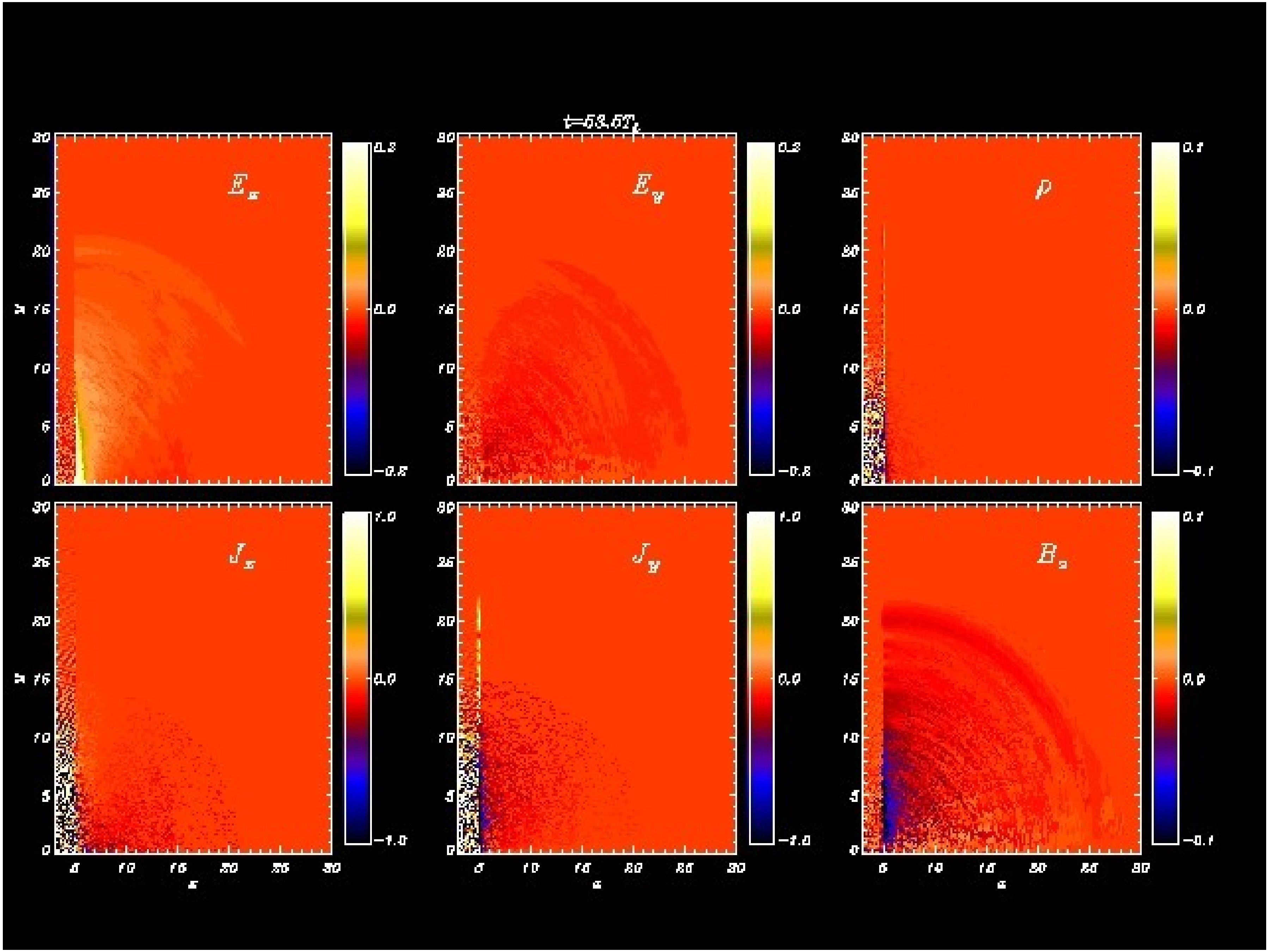

Field propagation on the rear surface of solid targets

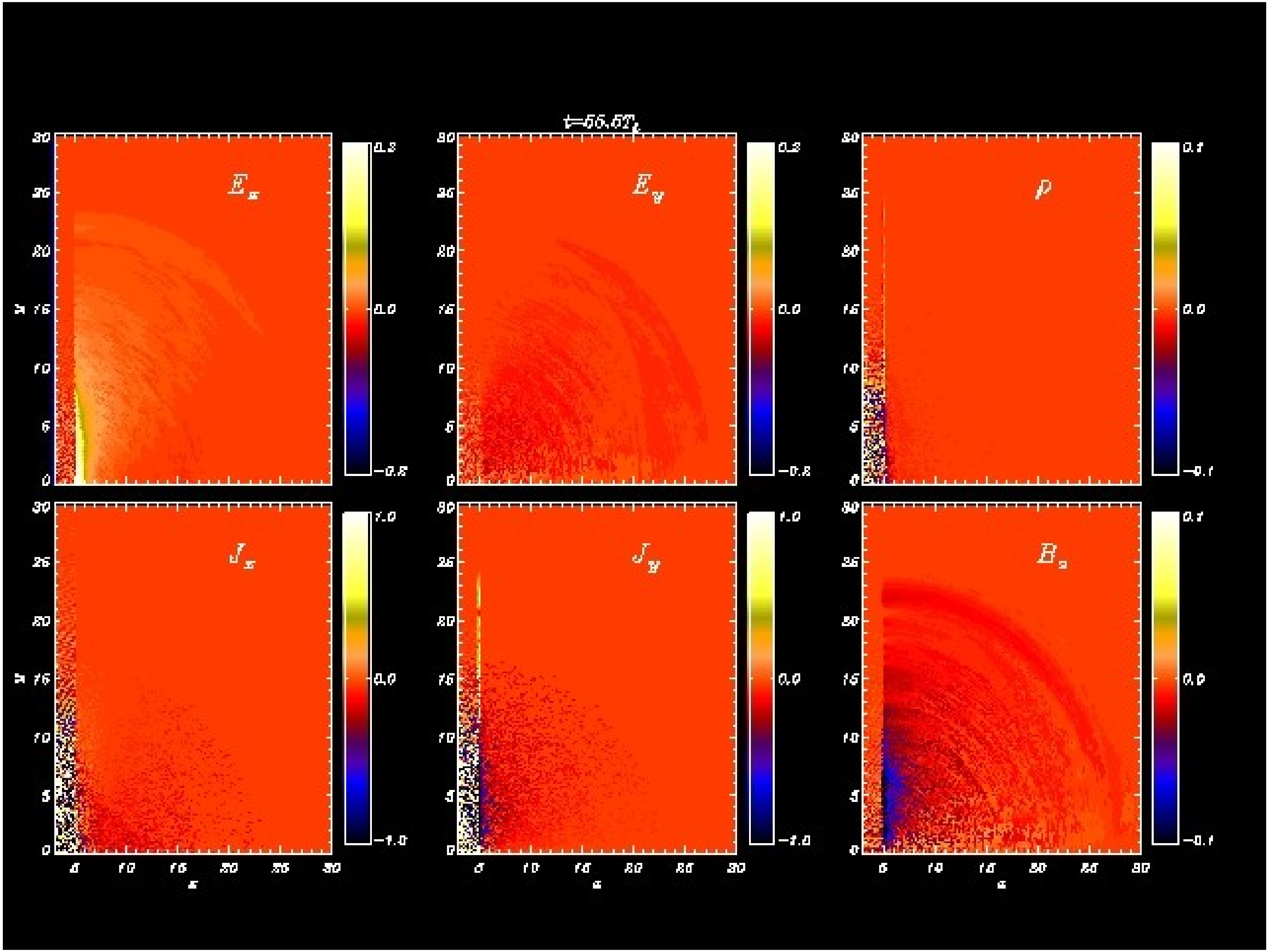

Field propagation on the rear surface of solid targets

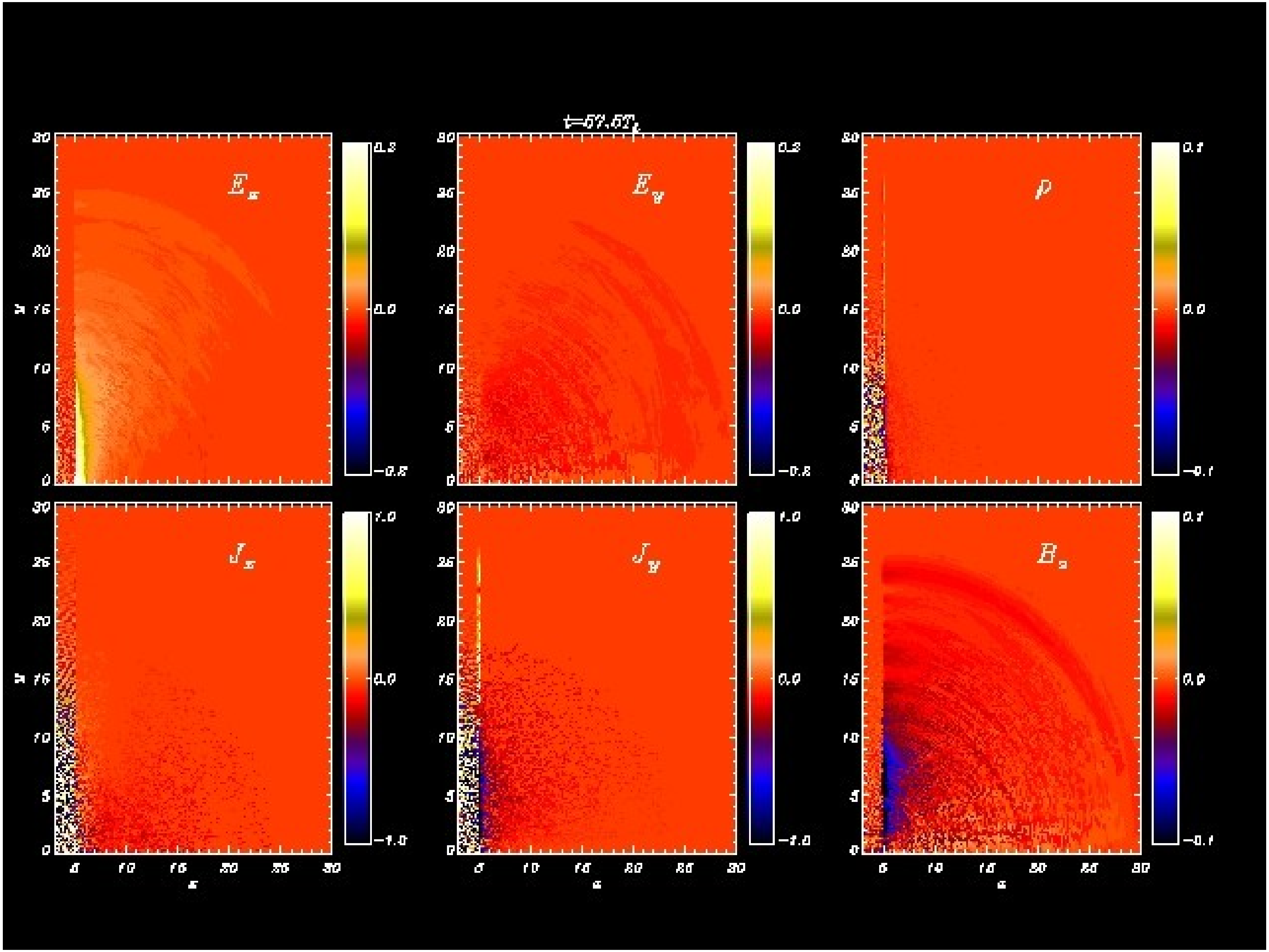

Field propagation on the rear surface of solid targets

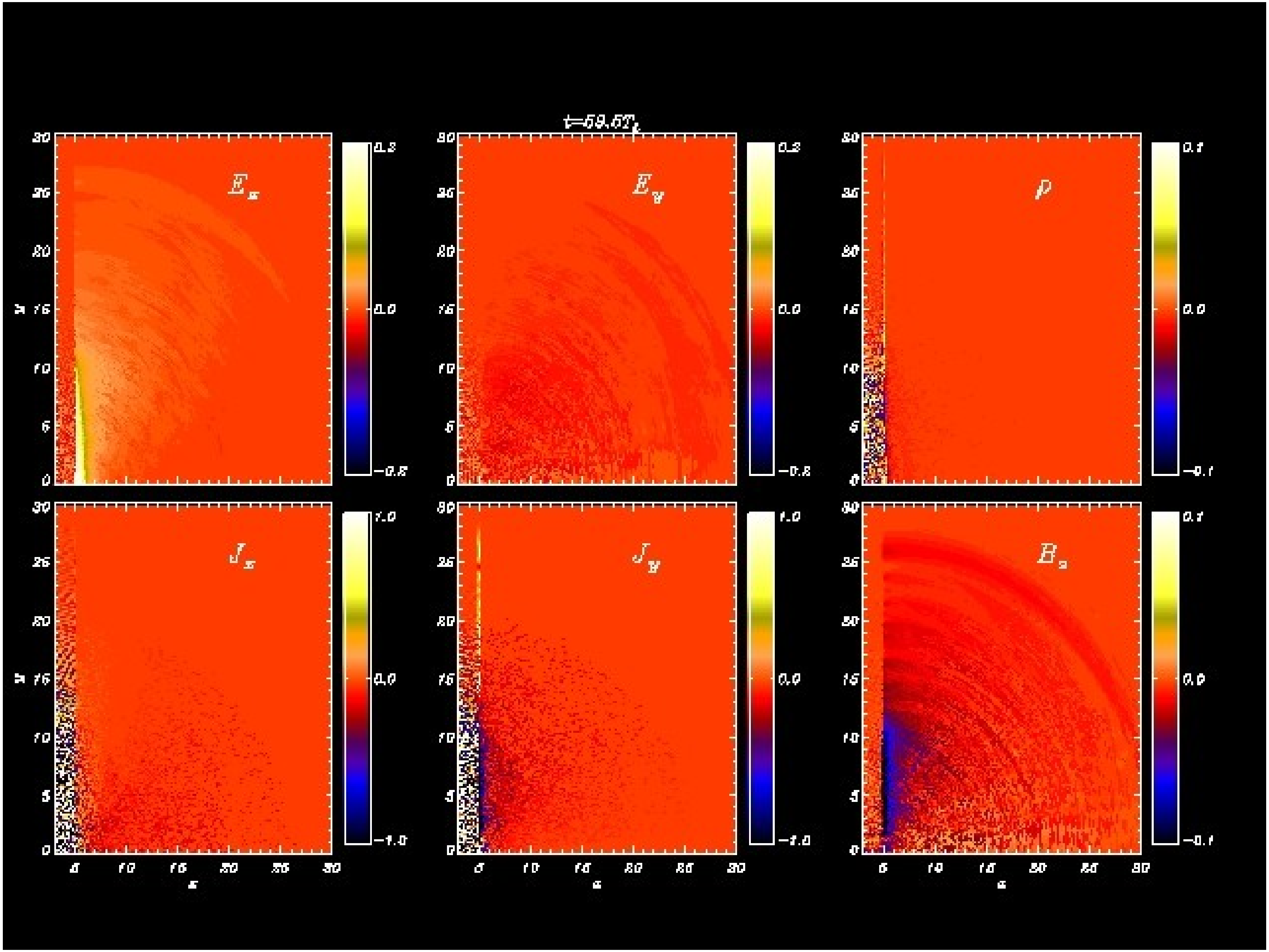

Field propagation on the rear surface of solid targets

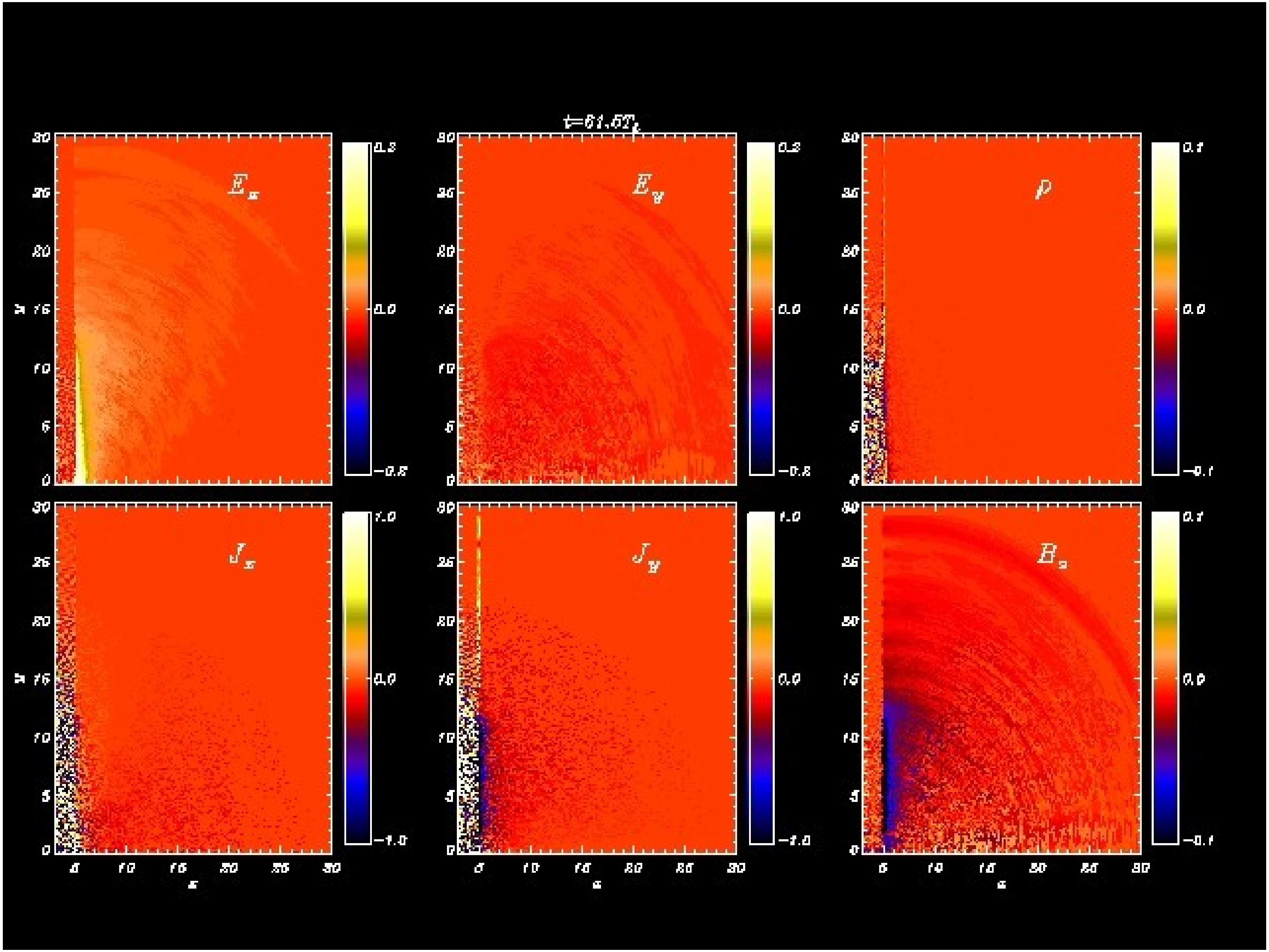

Conclusions

- The proton probing technique (PPT) with picosecond resolution allowed detailed studies of many relevant ultrafast phenomena in laser-plasma interactions for the first time, stimulating and challenging theoretical and computational work

- Noticeably, PPT improved our understanding of the physics of proton or ion acceleration itself

- Several additional phenomena may be investigated in the future, especially with laser systems allowing

• multiple beam probing

• higher ion energies (study of faster phenomena, probing of very dense plasmas)

This talk may be downloaded from

www.df.unipi.it/~macchi/talks.html

Electron probing of “colder” plasmas

Picosecond electron deflectometry of optical-field ionized plasmas

MARTIN CENTURION[1*†], PETER RECKENTHAELER[1,2†], SERGEI A. TRUSHIN[1], FERENC KRAUSZ[1,2] AND ERNST E. FILL[1]

[1]Max-Planck-Institut für Quantenoptik, Hans-Kopfermann-Strasse 1, D-85748 Garching, Germany
[2]Ludwig-Maximilians-Universität München, Am Coulombwall 1, D-85748 Garching, Germany

Nature Photonics **2** (2008) 315

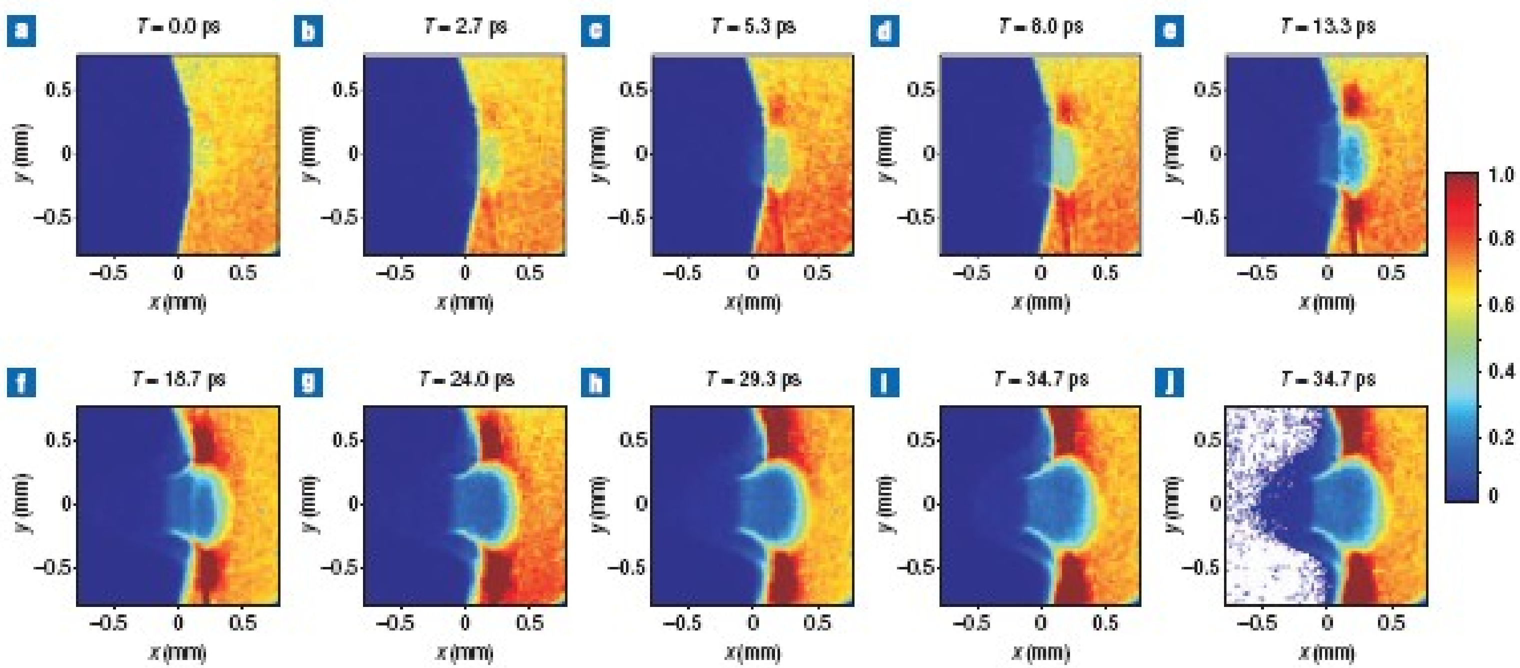

20 keV electrons suitable for measurements of $\boldsymbol{E}$ ~10^7-10^8 V/cm and $\boldsymbol{B}$ ~ 10^4 Gauss

Study of “coherent”, long-lived field structures

Theory and numerical simulations show that a variety of slowly varying structures (**solitons**, **vortices**, **cavitons** ...) is generated during laser-plasma interactions.

Bubble-like structures interpreted as remnants of **relativistic solitons** (“post-solitons”)

[Borghesi et al., Phys. Rev. Lett. **88** (2002) 135002]

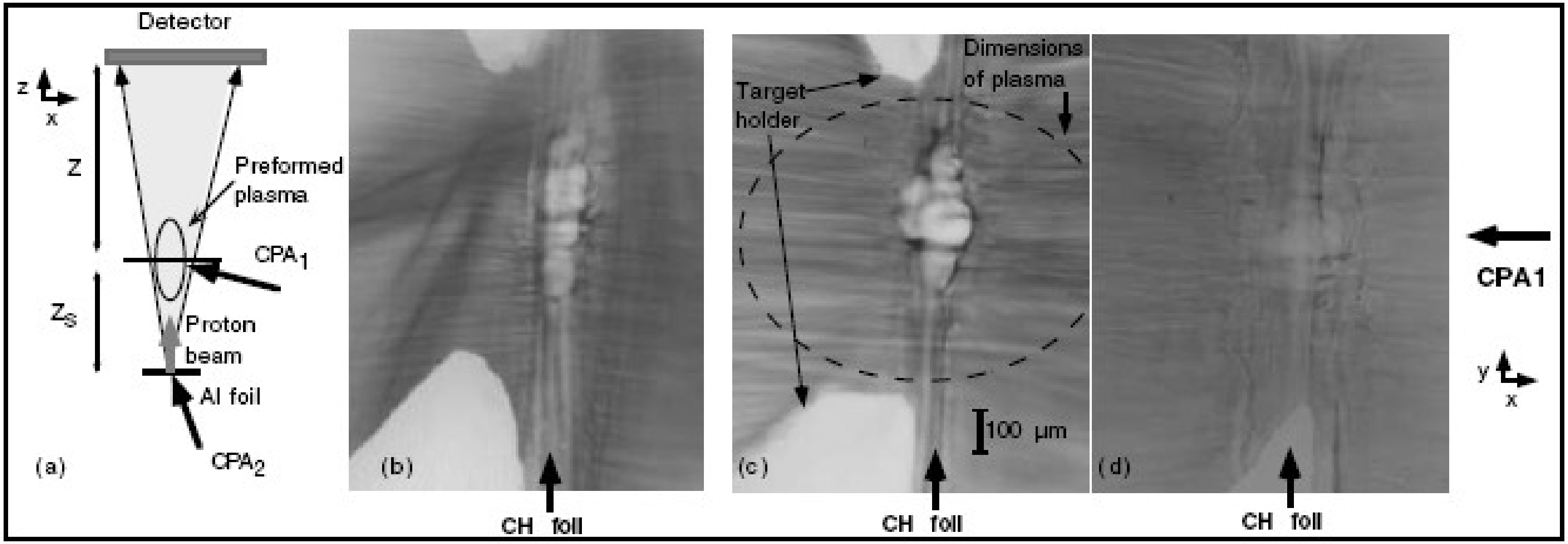

FIG. 1. (a) Experimental arrangement. (b), (c), (d) Proton images of the preformed plasma taken with 6–7 MeV protons, respectively: (b) 25 ps; (c) 45 ps; (d) 95 ps after the CPA_1 interaction. The scale refers to dimensions in the object plane. The dashed line indicates the dimensions of the preformed plasma defined by $n \approx 0.01 n_{cr}$ (at $\lambda = 1\ \mu$m).

Study of “coherent”, long-lived field structures

Theory and numerical simulations show that a variety of slowly varying structures (**solitons**, **vortices**, **cavitons** ...) is generated during laser-plasma interactions.

Ion modulations resulting from onset and evolution of **Buneman instability** in the late evolution of a plasma wake

[Borghesi et al., Phys. Rev. Lett. **94** (2005) 195003]

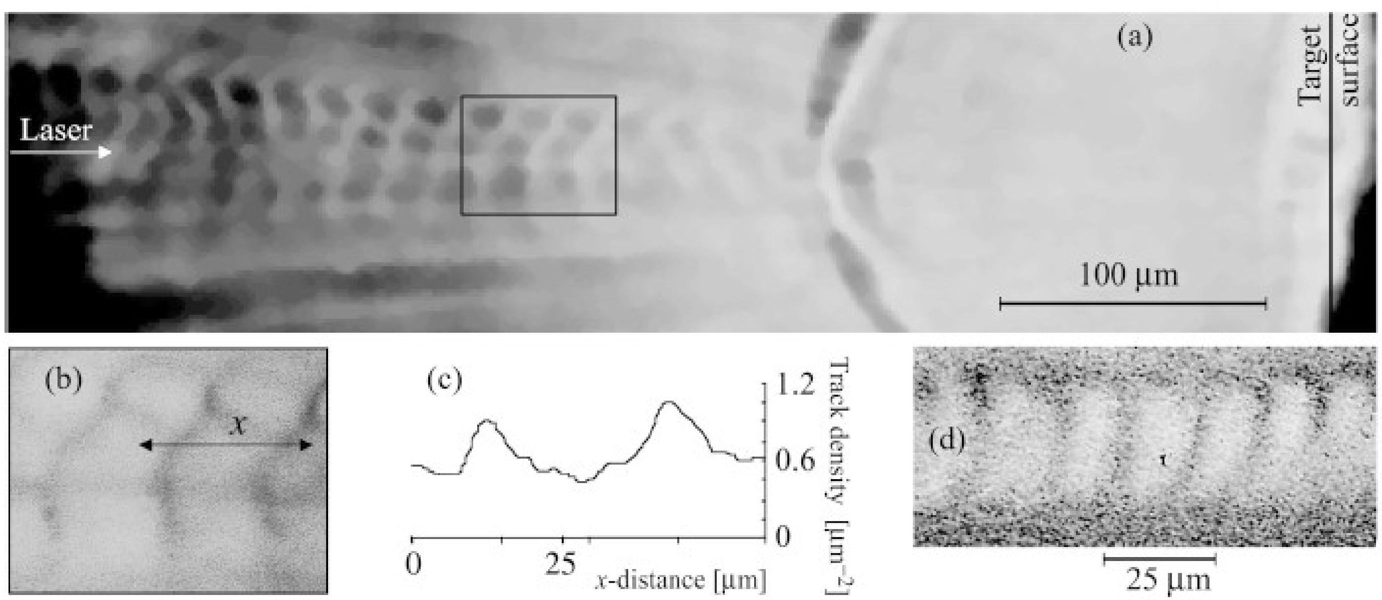

FIG. 1. (a) Proton projection image of the region in front of the laser-irradiated target, taken 20 ps after the interaction. The picture is a reflection scan of the exposed CR 39; (b) Detail of the image in frame (a), (c) Profile of the proton track density along the direction indicated by the arrow in (a); (d) Detail of the pattern observed at the back of a 0.9 μm Mylar target 20 ps after the interaction. The detail shown was located at a distance of about 200 μm from the original target plane.

Study of “coherent”, long-lived field structures

Theory and numerical simulations show that a variety of slowly varying structures (**solitons**, **vortices**, **cavitons** ...) is generated during laser-plasma interactions.

Regular, quasi-periodic structures observed inside or near the charge-displacement channel at late times

[T.V.Lyseikina, F.Ceccherini, F. Cornolti, E.Yu.Echkina, A.Macchi, F.Pegoraro, M.Borghesi, S.Kar, L.Romagnani, S.V.Bulanov, O.Willi, M.Galimberti, arXiv:physics/0701139]